

cally significant between untreated control and treated sample were selected.

Protein identification by mass spectrometry

For mass spectrometric analysis, 400 μg of unlabeled-protein extract was independently applied to 2D electrophoresis. The gel was stained with DeepPurple solution (GE Healthcare Bio-Sciences Corp.) according to the manufacturer's recommendation. The gel image was obtained by scanning with Ettan DIGE Primo and matched to those of analytical gels by using the ImageMaster 2D Platinum software. The spots of interest were picked out, and in-gel protein digestion was carried out with trypsin gold (Promega, Madison, WI, USA) as described.²⁶ Mass spectrometric analyses were performed by using a MALDI-TOF/TOF type mass spectrometer AB4700 (Applied Biosystems, Framingham, MA, USA). The proteins were identified through the online search using MASCOT database search engine.

Immunoblot analysis

The cell extracts obtained from cell cultures treated with or without HDACi were subjected to cell extract preparation as described above. The samples were applied to electrophoresis on a 10% polyacrylamide gel and transferred onto a nitrocellulose membrane. The membranes were incubated in TBS-T (10 mM Tris-HCl (pH, 8.0), 150 mM NaCl, 0.1% Tween) with 5% non-fat milk containing 1:1000 diluted primary antibodies against either caspase-9, -8, -7, -3, poly-ADP ribose polymerase (PARP) (Cell Signaling Technology, Danvers, MA, USA), peroxiredoxin 1 (Affinity Bioreagents, Golden, CO, USA), elongation factor-2 or α -tubulin (Santa Cruz, Santa Cruz, CA, USA). Membranes were then rinsed in TBS-T and further incubated with HRP-conjugated secondary antibody (GE Healthcare Bio-Sciences Corp.) in TBS-T with 5% non-fat milk. Each protein was detected by SuperSignal (PIERCE, Rockford, IL, USA).

Detection of ROS

ROS content was measured as described previously.²⁷ After treatment with HDACi, the cells were incubated with an oxidation-sensitive fluorescent probe 2', 7'-dichlorofluorescein diacetate (H_2 -DCFDA) (Molecular Probes Inc., Eugene, OR, USA) at a final concentration of 5 μM for 30 min. The cells were washed and resuspended in PBS, and then ROS amount was measured by flowcytometry.

Results

NCH-51 induces apoptosis greater than SAHA

We first evaluated the growth inhibitory effects of NCH-51 on a variety of lymphoid malignant cell lines (Figure 1a). A tentative result in a multiple myeloma cell line U266 cells is shown in Figure 1b. In most of the cell lines including U266 cells, NCH-51 exhibited a stronger growth inhibitory effect than SAHA at 3 μM for 24 h treatment, whereas prolonged incubation for 72 h did not show such a difference. It is noted that there was no significance in the growth inhibitory effect on four healthy donor PBMCs between NCH-51 and SAHA (IC_{50} values of both agents were higher than 30 μM), suggesting a cell-type specific cytotoxicity of NCH-51. We then analyzed the apoptosis and cell cycle distribution after the treatment with NCH-51 or SAHA. In the six cell lines (Jurkat, ED-40515(-), MEC2, U266, XG7 and ILKM-2), all of which showed a high susceptibility to

NCH-51 ($\text{IC}_{50} < 3 \mu\text{M}$), NCH-51 strongly induced apoptosis greater than SAHA after 24 h treatment as demonstrated by generation of sub- G_1 cells (Figure 1c and Table 1). In fact, when U266 cells were treated with NCH-51, cleaved forms of caspase-9, -8, -3 and PARP could be detected after 8 h, evidently at 16 h, although no activation of caspase-7 was detected (Figure 1d), suggesting that NCH-51 induces apoptosis through both extrinsic (type I) and intrinsic (type II) pathways²⁸ in the short-term treatment. On the other hand, cell cycle analysis revealed that NCH-51 increased the cell number at G_2/M -phase and reduced the number at G_1 - or S-phase in most of the cell lines examined (Table 1, right column). No significant difference in the effects on cell cycle regulation was observed between NCH-51- and SAHA-treated cells. These observations suggest that the apoptosis-inducing activity might be attributable to the difference in the observed growth inhibitory effects between NCH-51 and SAHA.

NCH-51 regulates the expressions of antioxidant molecules at the protein level

To identify the target molecules regulated by NCH-51, we analyzed the RNA and protein expression profiles. cDNA microarray analysis using U266 cells showed that NCH-51 treatment upregulated the expression of *p21* and *p19* (Supplementary Table 1), confirming the previous reports by us¹¹ and others.¹²⁻¹⁴ On the other hand, NCH-51 downregulated the gene expression of *CFLAR* (*c-FLIP*), *survivin* and *BCL2L2* (*bcl-w*), which act as antiapoptotic molecules. These results suggested that these genes were responsible for the growth inhibitory action of NCH-51, however, there was no notable difference in mRNA expression between NCH-51- and SAHA-treated cells. We then performed the proteome analysis. Whole cell extracts were prepared from U266 cells treated with or without NCH-51, and the protein samples were labeled with fluorescent dyes and applied to 2D electrophoresis (Figure 2a). By comparing the amounts of cellular proteins, we identified 14 proteins that varied relatively to NCH-51 treatment (Table 2). Ten proteins including nucleotide diphosphate kinase A (NDPKA), peroxiredoxin 1 and 2 (PRDX1, 2), glutathione S-transferase P1-1 (GSTP1-1), 14-3-3 zeta/delta, Cl^- intracellular channel proteins 1 and 4 (CLIC1, 4), proteasome subunit $\alpha 3$, protease activator 28 β subunit and Rho GDI α were upregulated, and four proteins including alanyl-tRNA synthetase (AARS), elongation factor-2 (EF-2), heat-shock 70 kDa protein 8 (HSPA8) and mitochondrial inner membrane protein, were downregulated after the treatment with NCH-51. Interestingly, some of these proteins upregulated by NCH-51 belong to a class of antioxidant molecules. It is noted that PRDX1 and PRDX2 were upregulated at both mRNA and protein levels, thus they are considered to be upregulated at the gene expression level, whereas most of the proteins were upregulated without induction at the gene expression level. In contrast, EF-2 and HSPA8 were downregulated at the protein level. The effects of NCH-51 and SAHA on the expression of EF-2 and PRDX1 were then verified. As shown in Figure 2b, EF-2 protein level was decreased either by NCH-51 or SAHA in the cell lines such as U266, ED-40515 (-) and XG7 cells that were highly susceptible to HDACi. EF-2 was decreased after 16 h treatment with these HDACi (data not shown). On the other hand, in the cell lines such as MEC2, Daudi and KM5 cells that were less sensitive to HDACi, EF-2 protein level was not significantly changed. PRDX1 protein level was upregulated by the treatment with either NCH-51 or SAHA in ED-40515 (-), U266, XG7 and MEC2 cells. SAHA seemed to upregulate PRDX1 more than NCH-51.

Table 1 The profiles of apoptosis and cell cycle distribution

Cell line	HDAC inhibitor (μM)	Apoptotic cell ^a (%)	Cell cycle distribution ^a (%)			
			sub G ₁	G ₁	S	G ₂ /M
Jurkat	Untreated control	6.30	5.11	50.39	20.76	20.64
	SAHA					
	3 μM	13.45	28.56	9.15	12.97	46.22
	30 μM	28.97	32.39	7.06	18.10	40.83
	NCH-51					
	3 μM	19.27	42.66	8.05	10.04	36.28
	30 μM	35.45	42.69	7.64	14.41	32.21
MT-2	Untreated control	6.84	3.02	63.25	15.29	15.64
	SAHA					
	3 μM	8.23	9.41	49.04	11.70	26.36
	30 μM	8.75	10.35	62.95	6.15	13.96
	NCH-51					
	3 μM	8.45	3.26	62.21	16.34	16.53
	30 μM	8.62	5.38	71.64	8.35	12.22
ED-40515 (-)	Untreated control	6.44	8.40	46.82	23.30	19.67
	SAHA					
	3 μM	20.74	18.88	21.41	19.07	36.90
	30 μM	20.12	26.87	22.20	20.49	27.75
	NCH-51					
	3 μM	22.12	27.10	28.04	19.04	23.91
	30 μM	21.33	26.54	25.09	20.56	25.72
MEC2	Untreated control	3.20	5.66	60.06	19.96	12.16
	SAHA					
	3 μM	4.84	12.32	37.33	19.84	26.70
	30 μM	8.22	18.14	29.46	22.63	25.12
	NCH-51					
	3 μM	6.50	16.22	36.43	19.28	24.75
	30 μM	11.08	21.24	30.47	20.93	23.29
MO1043	Untreated control	4.14	0.89	54.88	20.75	17.87
	SAHA					
	3 μM	4.30	3.45	68.83	7.49	15.41
	30 μM	15.96	18.85	48.29	6.62	23.14
	NCH-51					
	3 μM	3.74	2.47	73.90	7.17	12.88
	30 μM	14.93	21.75	48.79	6.14	21.03
Daudi	Untreated control	1.62	1.62	52.02	22.77	19.55
	SAHA					
	3 μM	2.08	2.17	23.65	22.33	46.30
	30 μM	2.12	2.34	22.83	19.75	48.21
	NCH-51					
	3 μM	2.64	1.90	50.38	14.74	27.71
	30 μM	3.04	2.19	25.68	22.19	43.28
U266	Untreated control	6.17	6.30	67.42	10.99	13.02
	SAHA					
	3 μM	17.65	11.91	56.24	10.35	19.72
	30 μM	29.73	17.06	48.70	12.69	19.68
	NCH-51					
	3 μM	22.90	13.39	54.07	11.60	18.62
	30 μM	32.63	18.90	49.15	13.40	18.94
XG7	Untreated control	7.27	7.58	49.21	20.34	23.37
	SAHA					
	3 μM	8.74	8.50	50.40	8.33	28.32
	30 μM	9.43	15.38	34.23	15.10	28.21
	NCH-51					
	3 μM	11.47	10.00	49.32	8.62	28.62
	30 μM	13.13	17.87	35.44	14.67	27.93
KM5	Untreated control	4.24	2.91	42.15	27.85	23.43
	SAHA					
	3 μM	4.30	6.32	31.85	31.44	26.13
	30 μM	15.96	23.37	20.62	26.19	24.68
	NCH-51					
	3 μM	3.74	6.75	38.34	29.96	20.84
	30 μM	18.46	20.33	27.77	23.29	24.31

Table 1 (Continued)

Cell line	HDAC inhibitor (μM)	Apoptotic cell ^a (%)	Cell cycle distribution ^a (%)			
			sub G ₁	G ₁	S	G ₂ /M
ILKM-2	Untreated control	7.35	4.07	58.61	13.05	22.89
	SAHA					
	3 μM	7.84	8.97	61.53	6.23	22.12
	30 μM	21.41	20.63	51.10	12.71	13.88
	NCH-51					
	3 μM	8.71	6.04	63.21	6.93	22.45
	30 μM	30.04	20.54	51.45	12.15	15.13

Abbreviations: HDAC, histone deacetylase; SAHA, suberoylanilide hydroxamic acid.
^aEach value shows the average of 20000 cells counted.

NCH-51 induces cytotoxic effect through the modulation of intracellular ROS

From the results of proteome analyses, NCH-51 appeared to promote the expression of antioxidant molecules, either at the transcriptional or post-transcriptional level, which prompted us to examine the effect of NCH-51 on the levels of ROS accumulation. Interestingly, the temporal profile of ROS amount in U266 cells treated with NCH-51 appeared to be in a concave shape indicating a gradual suppression of ROS accumulation within the initial 4 h and subsequent induction of ROS (Figure 3a), whereas the temporal profile with SAHA continuously declined over time. Similar trends were observed with other cell lines (data not shown). As summarized in Table 2, SAHA was more effective in reducing ROS than NCH-51, and the difference in ROS amount between NCH-51 and SAHA was most evident at 24 h, when the difference in growth inhibitory effect could be observed (Figure 1). These results suggested a possibility that dynamic state of ROS in each cell could be attributed to the growth inhibitory effect of HDACi. We thus examined whether NAC, a small-molecule antioxidant compound, could modulate the effect of NCH-51 (Figure 3b). Expectedly, when U266 cells were pretreated with NAC, the NCH-51-mediated cell growth inhibition was abolished. Similar effect was observed in SAHA-treated cells as much as in NCH-51-treated cells (data not shown). These results indicated that high amount of ROS might be necessary for the induction of NCH-51-mediated cytotoxicity.

Discussion

There have been accumulating reports of successful inhibition of cancer cell growth using small-molecule HDACi compounds.^{1,7} Initial studies with SAHA indicated that the mode of action of HDACi might be through upregulating the transcriptionally repressed genes during carcinogenic processes by acetylating the repressive histones.¹²⁻¹⁴ However, recent reports have demonstrated that HDACi compounds also exert anticancer effects through acetylation of non-histone substrates.¹⁵⁻¹⁹ For example, HDAC6, a microtubule-associated deacetylase, was shown to be responsible for transportation of misfolded proteins to aggresomes thus promoting protein degradation.^{19,29} Thus, we have attempted to clarify the mechanism of anticancer effects of NCH-51 by examining both mRNA and protein levels.

In this study, we noticed that NCH-51 induced apoptosis in sensitive cell lines greater than SAHA (Figures 1 and 2a and Table 1). Analyses of mRNA expression levels in NCH-51- and SAHA-treated cells has revealed that transcriptional repression of antiapoptotic genes, such as *survivin*, *bcl-w* and *c-FLIP* and

upregulation of cell cycle regulators, such as *p21* and *p19*, could be attributable to the induction of apoptosis and cell cycle arrest, respectively (Supplementary Table 1, 2 and Supplementary Figure 1), supporting the previous findings by others.¹²⁻¹⁴ There was no difference in the mRNA expression level between NCH-51- and SAHA-treated samples (Supplementary Figure 1). We have confirmed no difference in inducing activity for acetylation of histone H4 between these two HDACi's (Supplementary Figure 2). These findings suggest that NCH-51 and SAHA similarly affect gene expression presumably through histone acetylation. We thus examined the effects of these compounds on protein expression profile to understand the difference between NCH-51 and SAHA at the post-transcriptional level.

Interestingly, our proteome analyses revealed the upregulation of some antioxidant molecules including PRDX1, PRDX2 and GSTP1-1 (Table 2 and Figure 2). In addition, previous reports indicated that some other proteins identified by the present proteome analysis (Table 2) could be activated by oxidative stress.³⁰⁻³⁴ For example, NDPKA is reported to be activated by ROS and protected the cell from ROS-induced apoptosis.^{30,31} CLIC1 protein contains a redox-active site and is activated during ROS-triggered apoptosis.^{32,33} These findings suggested a possibility that NCH-51 might induce the cytotoxic effect by modulating the intracellular ROS content. In fact, pretreatment with NAC abolished the growth inhibitory effect of NCH-51 (Figure 3b). These results support the previous findings by others, which showed the ROS accumulation by HDACi.^{14,34,35} However, in contrast to the previous reports, both NCH-51 and SAHA downregulated the ROS content after 24 h treatment in most of the cell lines tested except for KM5 cells, in which ROS was increased by the treatment with SAHA or NCH-51 (Table 3). These findings were reproducibly observed. Although we currently do not know the reason why there was a discrepancy between our study and others, we think the time-point and/or cell characteristics may be different between them. When temporal profiles of ROS accumulation were examined (Figure 3a), we found a typical bimodal kinetics of the intracellular ROS content after treatment with NCH-51; an initial downregulation and subsequent upregulation of ROS. On the other hand, SAHA did not follow the similar kinetics and the intracellular ROS level gradually and continuously decreased (Figure 3a). Therefore, it is possible that apparent differences in the ability of cell growth inhibition between NCH-51 and SAHA, may be explained through the different effects on the redox status of cells and induction of antioxidant proteins. Interestingly, our proteome/transcriptome analyses have revealed that the upregulation of antioxidant molecules occurred at either protein or mRNA levels: GSTP1-1 was upregulated by

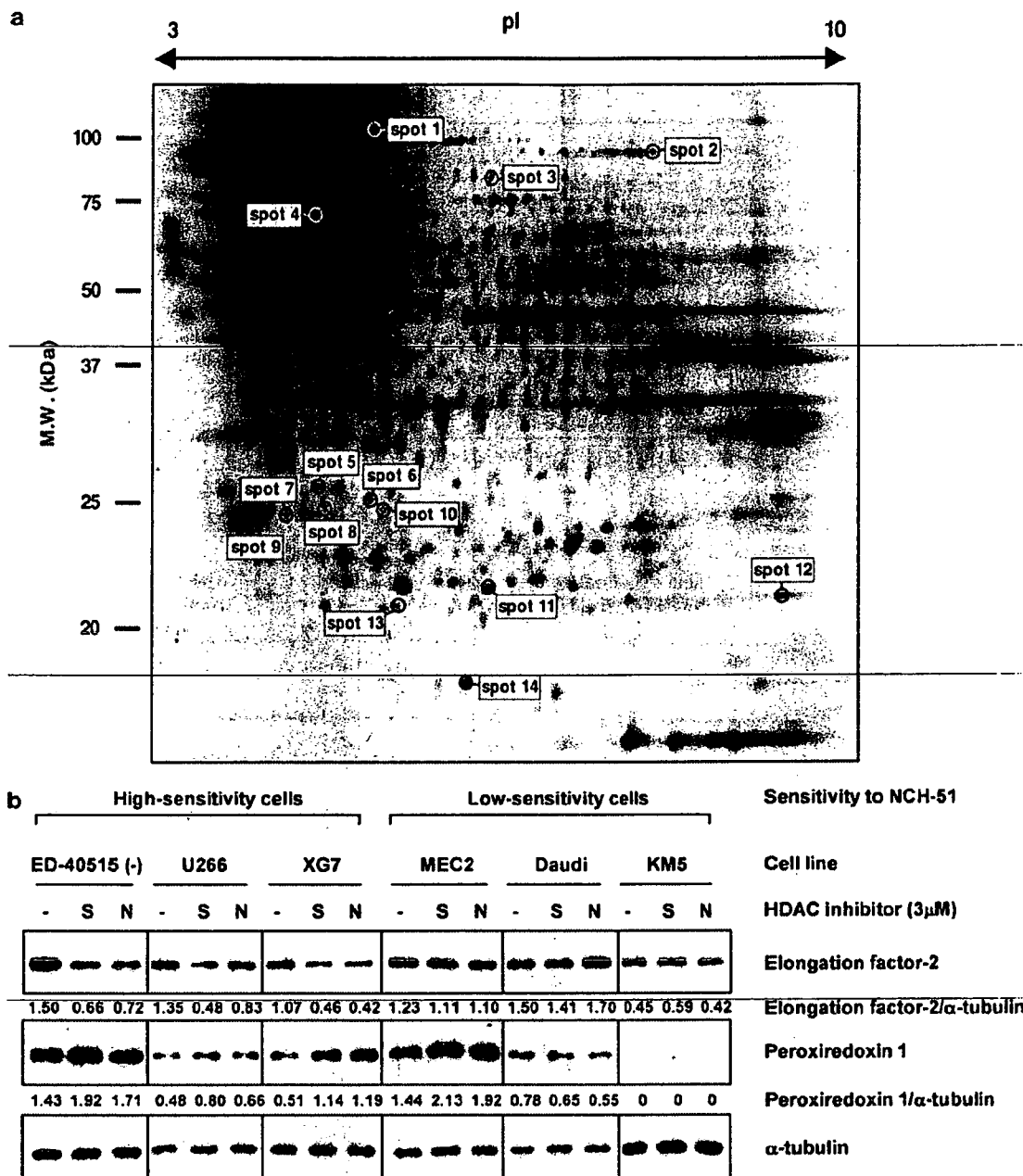


Figure 2 Proteome analysis of the effects of NCH-51. (a) 2D electrophoresis image of whole cell proteins prepared from U266 cells. After U266 cells were treated with or without 3 μ M NCH-51 for 18 h, the whole cell extracts were prepared and applied to 2D electrophoresis in quadruplicates. Fourteen spots, whose relative amounts were either increased or decreased by the treatment with NCH-51 in all four gels, were indicated. Each spot number in the image corresponds to those in Table 2. MW, molecular weight (kDa). pI, isoelectric point. (b) Downregulation of elongation factor-2 (EF-2) and upregulation of peroxiredoxin 1 (PRDX1) by HDACi. The cells were treated with suberoylanilide hydroxamic acid (S) or NCH-51 (N) (3 μ M) for 18 h. Whole cell extracts were prepared and subjected to immunoblots with the indicated antibodies. Each value means the ratio of the protein amount to α -tubulin (internal control).

NCH-51 only at the protein level, and PRDX1 and PRDX2 were upregulated primarily at the transcriptional level. These findings suggest that there may be two consequent antioxidative mechanisms by which HDACi modulate ROS accumulation: (i) the mRNA level, acting through induction of transcription of antioxidant molecules *de novo*, and (ii) the protein level, which was presumably caused by blocking the cellular protein transport/degradation pathway involving aggresome and proteasome. Importantly, we have observed that SAHA but not NCH-

51 could induce acetylations of α -tubulin and HSP90 (Supplementary Figure 2), suggesting that SAHA might prolong the latter mechanism through blocking the degradation of antioxidant molecules. In fact, SAHA seemed to increase protein expression of PRDX1 greater than NCH-51 (Figure 2b). Since NCH-51 does not retain antioxidant molecules at the protein level, it induces the accumulation of ROS. Cellular levels of antioxidant molecules have been reported to be associated with the sensitivity to conventional anticancer agents.³⁶ Therefore,

Table 2 Upregulated/downregulated proteins after the treatment with NCH-51 in U266 cells

Spot no.	Protein ID	Protein name	MW	pI	Protein ratio (T/C) ^a	mRNA ratio (T/C) ^a
1	NP_001596	Alanyl-tRNA synthetase (AARS)	106734	5.31	0.80	0.74
2	NP_001952	Elongation factor-2 (EF-2)	95146	6.42	0.82	1.23
3	NP_006830	Mitochondrial inner membrane protein (IMMT)	83626	6.08	0.83	0.64
4	NP_006588	Heat-shock 70 kDa protein 8 (HSPA8)	70854	5.28	0.82	1.18
5	NP_001279	Cl ⁻ intracellular channel protein 1 (CLIC1)	26775	5.09	1.34	0.67
6	NP_002809	Protease activator 28 β subunit (PA28β)	27213	5.44	1.54	1.03
7	NP_004300	Rho GDP-dissociation inhibitor 1 (Rho GDIα)	23193	5.02	1.42	0.92
8	NP_002779	Proteasome subunit α type3	28284	5.19	1.32	0.73
9	NP_663723	14-3-3 ζ/δ (PKC inhibitor protein 1)	28828	4.73	1.37	0.83
10	NP_039234	Cl intracellular channel protein 4 (CLIC4)	28754	5.45	1.38	0.86
11	NP_000843	Glutathione S-transferase P 1-1 (GSTP1-1)	23210	5.44	1.38	0.98
12	NP_002565	Peroxiredoxin 1 (thioredoxin peroxidase 2) (PRDX1)	22096	8.27	1.30	1.4
13	NP_005800	Peroxiredoxin 2 (thioredoxin peroxidase 1) (PRDX2)	21747	5.67	1.30	1.35
14	NP_000260	Nucleoside diphosphate kinase A (NDPKA)	17138	5.83	1.50	1.04

^aThe results are indicated as the ratio of NCH-51-treated sample to untreated control (T/C).

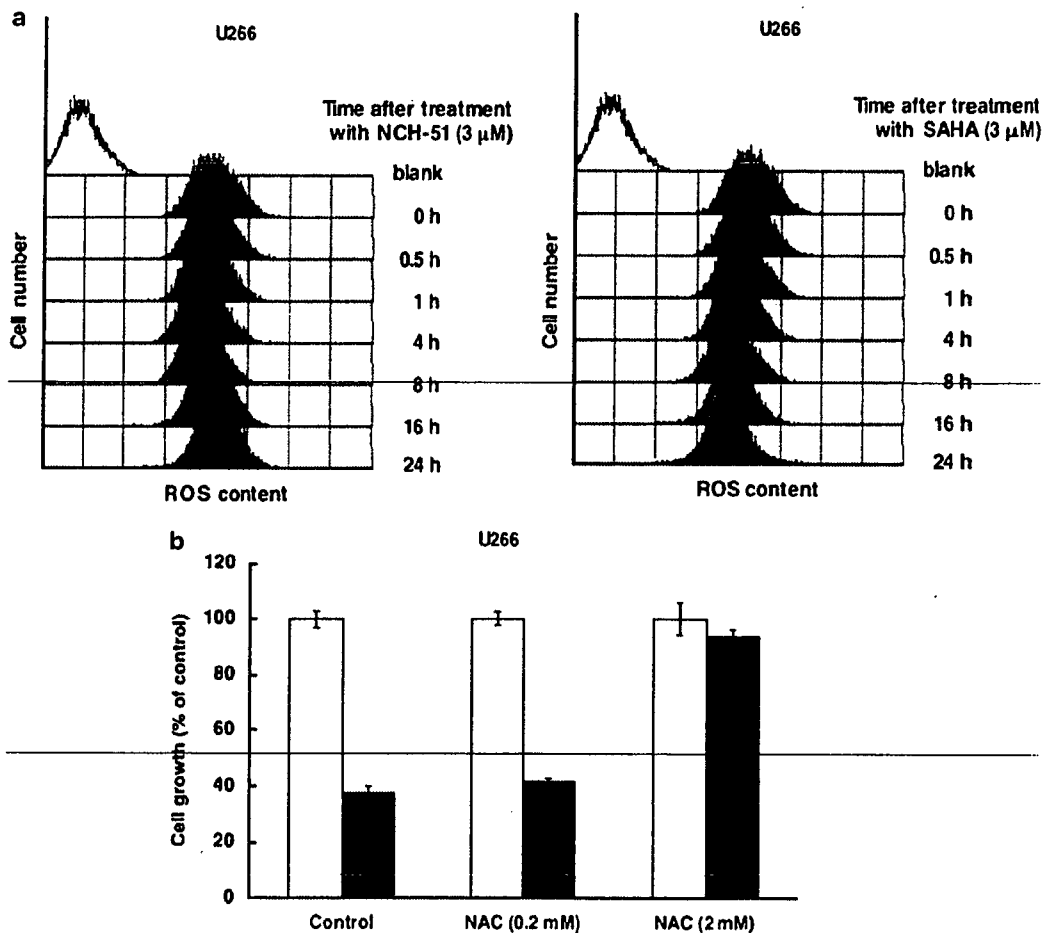


Figure 3 Effects of NCH-51 and suberoylanilide hydroxamic acid (SAHA) on reactive oxygen species (ROS) accumulation. (a) Time course of intracellular ROS after the treatment with HDACi. U266 cells were treated with NCH-51 or SAHA (3 μM) given the indicated time (0–24 h). After the treatment, H₂-DCFDA was added and further incubated for 30 min. ROS content was measured by flowcytometry. Blank, H₂-DCFDA-untreated control. (b) Effects of *N*-acetyl-L-cysteine (NAC) on the NCH-51-induced cell growth inhibition. U266 cells were treated with or without NCH-51 (3 μM) for 24 h in the presence or absence of NAC (0.2 or 2 mM). Cell growth was measured by 3-(4,5-dimethylthiazol-2-yl)-2,5-diphenyltetrazolium bromide assay. Open and closed bars indicate untreated and the NCH-51-treated cells. The results are shown as the percentage compared to untreated control. Experiments were done in triplicates and the mean values ±s.d. are shown.

NCH-51 can not only induce apoptosis through ROS accumulation, but also enhance the cytotoxicity of other agents in the combination treatment more efficiently than SAHA.

Our proteome analysis has also identified several proteins other than antioxidant molecules, including EF-2, AARS and HSPA8. We confirmed that EF-2 protein, a member of the GTP-

Table 3 ROS content and growth inhibitory effect after the treatment with HDAC inhibitor

Cell line	ROS content (% of control) ^a		Growth inhibition (% of control) ^b	
	NCH-51 (3 μM)	SAHA (3 μM)	NCH-51 (3 μM)	SAHA (3 μM)
Jurkat	86	47	63.5 ± 0.8	37.7 ± 2.5
MT-2	100	100	38.8 ± 0.3	11.0 ± 2.3
ED-40515 (-)	82	56	71.2 ± 1.2	44.1 ± 1.0
MEC2	59	46	41.3 ± 1.1	3.5 ± 2.8
MO1043	91	65	46.0 ± 0.5	7.2 ± 2.9
Daudi	74	54	25.6 ± 1.8	15.1 ± 3.0
U266	95	85	80.7 ± 1.8	51.7 ± 3.2
XG7	74	28	66.5 ± 1.1	23.1 ± 1.6
KM5	126	119	20.5 ± 0.5	14.6 ± 1.2
ILKM-2	94	94	85.5 ± 0.2	81.3 ± 1.1

Abbreviations: HDAC, histone deacetylase; ROS, reactive oxygen species; SAHA, suberoylanilide hydroxamic acid.

^aEach value shows the average of 20 000 cells counted.

^bEach value shows the mean ± s.d.

binding translational elongation factor family,³⁷ was specifically decreased in high-sensitivity cell lines such as ED-40515 (-) and U266 cells (Figure 2b) after 16 h treatment (data not shown). However, gene expression of EF-2 was upregulated after the treatment with NCH-51 (Table 2). This discrepancy indicates a possibility that NCH-51 could induce rapid turnover of EF-2 protein followed by upregulation of RNA expression. Similar effects on EF-2 were also observed with SAHA (Figure 2b). Since EF-2 has been reported to be inactivated by ROS and lead to inhibition of translation,³⁸ it is suggested that locally induced ROS by HDACi might induce EF-2 inactivation and degradation presumably by direct oxidation. Although the mechanism by which EF-2 is downregulated by HDACi remains unclear, EF-2 may be used as a feasible surrogate marker to evaluate the susceptibility of HDACi. Similar to EF-2, AARS and HSPA8 were downregulated at the protein level. It is known that HSPA8 are involved in protein folding and transport.³⁹ Thus, these findings collectively suggest that NCH-51 might arrest protein synthesis and transportation.

In conclusion, our study demonstrates the therapeutic advantage of NCH-51 on growth inhibition of lymphoid malignant cells. Importantly, NCH-51 did not affect the cell growth of normal PBMCs with the effective concentrations on malignant cells (Figure 1b). In addition to its therapeutic efficacy and selectivity, NCH-51 has additional advantages in clinical use based on its pharmacological features. Therefore, NCH-51 could be a useful anticancer agent against lymphoid malignancies.

Acknowledgements

We thank Mr ME Cueno for language editing. This work is supported in part by grant-in-aids from the Ministry of Education, Culture, Sports, Science and Technology and the Ministry of Health, Labor and Welfare of Japan. TS is supported by a grant of Aichi Cancer Research Foundation and a grant of Oujinkai Foundation. HN, TS and NY are supported by a grant of Takeda Science Foundation.

References

1 Minucci S, Pelicci PG. Histone deacetylase inhibitors and the promise of epigenetic (and more) treatments for cancer. *Nat Rev Cancer* 2006; **6**: 38–51.

2 Strahl BD, Allis CD. The language of covalent histone modifications. *Nature* 2000; **403**: 41–45.

3 Turner BM. Cellular memory and the histone code. *Cell* 2002; **111**: 285–291.

4 Claus R, Lubbert M. Epigenetic targets in hematopoietic malignancies. *Oncogene* 2003; **22**: 6489–6496.

5 Fraga MF, Ballestar E, Villar-Garea A, Boix-Chornet M, Espada J, Schotta G et al. Loss of acetylation at Lys16 and trimethylation at Lys20 of histone H4 is a common hallmark of human cancer. *Nat Genet* 2005; **37**: 391–400.

6 Seligson DB, Horvath S, Shi T, Yu H, Tze S, Grunstein M et al. Global histone modification patterns predict risk of prostate cancer recurrence. *Nature* 2005; **435**: 1262–1266.

7 Kelly WK, Marks PA. Drug insight: histone deacetylase inhibitors—development of the new targeted anticancer agent suberoylanilide hydroxamic acid. *Nat Clin Pract Oncol* 2005; **2**: 150–157.

8 Kelly WK, O'Connor OA, Krug LM, Chiao JH, Heaney M, Curley T et al. Phase I study of an oral histone deacetylase inhibitor, suberoylanilide hydroxamic acid, in patients with advanced cancer. *J Clin Oncol* 2005; **23**: 3923–3931.

9 Ryan QC, Headlee D, Acharya M, Sparreboom A, Trepel JB, Ye J et al. Phase I and pharmacokinetic study of MS-275, a histone deacetylase inhibitor, in patients with advanced and refractory solid tumors or lymphoma. *J Clin Oncol* 2005; **23**: 3912–3922.

10 Golub LM, Lee HM, Ryan ME, Giannobile WV, Payne J, Sorsa T. Tetracyclines inhibit connective tissue breakdown by multiple non-antimicrobial mechanisms. *Adv Dent Res* 1998; **12**: 12–26.

11 Suzuki T, Nagano Y, Kouketsu A, Matsuura A, Maruyama S, Kurotaki M et al. Novel inhibitors of human histone deacetylases: design, synthesis, enzyme inhibition, and cancer cell growth inhibition of SAHA-based non-hydroxamates. *J Med Chem* 2005; **48**: 1019–1032.

12 Huang L, Sowa Y, Sakai T, Pardee AB. Activation of the p21WAF1/CIP1 promoter independent of p53 by the histone deacetylase inhibitor suberoylanilide hydroxamic acid (SAHA) through the Sp1 sites. *Oncogene* 2000; **19**: 5712–5719.

13 Richon VM, Sandhoff TW, Rifkind RA, Marks PA. Histone deacetylase inhibitor selectively induces p21WAF1 expression and gene-associated histone acetylation. *Proc Natl Acad Sci USA* 2000; **97**: 10014–10019.

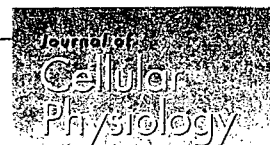
14 Rosato RR, Almenara JA, Grant S. The histone deacetylase inhibitor MS-275 promotes differentiation or apoptosis in human leukemia cells through a process regulated by generation of reactive oxygen species and induction of p21CIP1/WAF1. *Cancer Res* 2003; **63**: 3637–3645.

15 Bali P, Prnpat M, Bradner J, Balasis M, Fiskus W, Guo F et al. Inhibition of histone deacetylase 6 acetylates and disrupts the chaperone function of heat shock protein 90: a novel basis for antileukemia activity of histone deacetylase inhibitors. *J Biol Chem* 2005; **280**: 26729–26734.

16 Hubbert C, Guardiola A, Shao R, Kawaguchi Y, Ito A, Nixon A et al. HDAC6 is a microtubule-associated deacetylase. *Nature* 2002; **417**: 455–458.

- 17 Insinga A, Monestiroli S, Ronzoni S, Carbone R, Pearson M, Pruneri G *et al*. Impairment of p53 acetylation, stability and function by an oncogenic transcription factor. *EMBO J* 2004; **23**: 1144–1154.
- 18 Chen L, Fischle W, Verdin E, Greene WC. Duration of nuclear NF-kappaB action regulated by reversible acetylation. *Science* 2001; **293**: 1653–1657.
- 19 Hideshima T, Bradner JE, Wong J, Chauhan D, Richardson P, Schreiber SL *et al*. Small-molecule inhibition of proteasome and aggresome function induces synergistic antitumor activity in multiple myeloma. *Proc Natl Acad Sci USA* 2005; **102**: 8567–8572.
- 20 Sanda T, Asamitsu K, Ogura H, Iida S, Utsunomiya A, Ueda R *et al*. Induction of cell death in adult T-cell leukemia cells by a novel IkappaB kinase inhibitor. *Leukemia* 2006; **20**: 590–598.
- 21 Uranishi M, Iida S, Sanda T, Ishida T, Tajima E, Ito M *et al*. Multiple myeloma oncogene 1 (MUM1)/interferon regulatory factor 4 (IRF4) upregulates monokine induced by interferon-gamma (MIC) gene expression in B-cell malignancy. *Leukemia* 2005; **19**: 1471–1478.
- 22 Pulvertaft JV. Cytology of Burkitt's tumour (African lymphoma). *Lancet* 1964; **39**: 238–240.
- 23 Klein E, Klein G, Nadkarni JS, Nadkarni JJ, Wigzell H, Clifford P. Surface IgM-kappa specificity on a Burkitt lymphoma cell *in vivo* and in derived culture lines. *Cancer Res* 1968; **28**: 1300–1310.
- 24 Suzuki A, Iida S, Kato-Uranishi M, Tajima E, Zhan F, Hanamura I *et al*. ARK5 is transcriptionally regulated by the Large-MAF family and mediates IGF-1-induced cell invasion in multiple myeloma: ARK5 as a new molecular determinant of malignant multiple myeloma. *Oncogene* 2005; **24**: 6936–6944.
- 25 Sanda T, Iida S, Ogura H, Asamitsu K, Murata T, Bacon KB *et al*. Growth inhibition of multiple myeloma cells by a novel IkappaB kinase inhibitor. *Clin Cancer Res* 2005; **11**: 1974–1982.
- 26 Seike M, Kondo T, Mori Y, Gemma A, Kudoh S, Sakamoto M *et al*. Proteomic analysis of intestinal epithelial cells expressing stabilized beta-catenin. *Cancer Res* 2003; **63**: 4641–4647.
- 27 Imai K, Nakata K, Kawai K, Hamano T, Mei N, Kasai H *et al*. Induction of OGG1 gene expression by HIV-1 Tat. *J Biol Chem* 2005; **280**: 26701–26713.
- 28 Opferman JT, Korsmeyer SJ. Apoptosis in the development and maintenance of the immune system. *Nat Immunol* 2003; **4**: 410–415.
- 29 Kawaguchi Y, Kovacs JJ, McLaurin A, Vance JM, Ito A, Yao TP. The deacetylase HDAC6 regulates aggresome formation and cell viability in response to misfolded protein stress. *Cell* 2003; **115**: 727–738.
- 30 Song EJ, Kim YS, Chung JY, Kim E, Chae SK, Lee KJ. Oxidative modification of nucleoside diphosphate kinase and its identification by matrix-assisted laser desorption/ionization time-of-flight mass spectrometry. *Biochemistry* 2000; **39**: 10090–10097.
- 31 Arnaud-Dabernat S, Masse K, Smani M, Peuchant E, Landry M, Bourbon PM *et al*. Nm23-M2/NDP kinase B induces endogenous c-myc and nm23-M1/NDP kinase A overexpression in BAF3 cells. Both NDP kinases protect the cells from oxidative stress-induced death. *Exp Cell Res* 2004; **301**: 293–304.
- 32 Harrop SJ, DeMaere MZ, Fairlie WD, Reztsova T, Valenzuela SM, Mazzanti M *et al*. Crystal structure of a soluble form of the intracellular chloride ion channel CLIC1 (NCC27) at 1.4-Å resolution. *J Biol Chem* 2001; **276**: 44993–45000.
- 33 Shimizu T, Numata T, Okada Y. A role of reactive oxygen species in apoptotic activation of volume-sensitive Cl(−) channel. *Proc Natl Acad Sci USA* 2004; **101**: 6770–6773.
- 34 Ruefli AA, Ausserlechner MJ, Bernhard D, Sutton VR, Tainton KM, Kofler R *et al*. The histone deacetylase inhibitor and chemotherapeutic agent suberoylanilide hydroxamic acid (SAHA) induces a cell-death pathway characterized by cleavage of Bid and production of reactive oxygen species. *Proc Natl Acad Sci USA* 2001; **98**: 10833–10838.
- 35 Ungerstedt JS, Sowa Y, Xu WS, Shao Y, Dokmanovic M, Perez C *et al*. Role of thioredoxin in the response of normal and transformed cells to histone deacetylase inhibitors. *Proc Natl Acad Sci USA* 2005; **102**: 673–678.
- 36 Yokomizo A, Ono M, Nanri H, Makino Y, Ohga T, Wada M *et al*. Cellular levels of thioredoxin associated with drug sensitivity to cisplatin, mitomycin C, doxorubicin, and etoposide. *Cancer Res* 1995; **55**: 4293–4296.
- 37 Ryazanov AG, Shestakova EA, Natapov PG. Phosphorylation of elongation factor 2 by EF-2 kinase affects rate of translation. *Nature* 1988; **334**: 170–173.
- 38 Patel J, McLeod LE, Vries RG, Flynn A, Wang X, Proud CG. Cellular stresses profoundly inhibit protein synthesis and modulate the states of phosphorylation of multiple translation factors. *Eur J Biochem* 2002; **269**: 3076–3085.
- 39 Young JC, Agashe VR, Siegers K, Hartl FU. Pathways of chaperone-mediated protein folding in the cytosol. *Nat Rev Mol Cell Biol* 2004; **5**: 781–791.

Supplementary Information accompanies the paper on the Leukemia website (<http://www.nature.com/leu>)



Granulocyte Colony-Stimulating Factor Promotes the Translocation of Protein Kinase C ζ in Neutrophilic Differentiation Cells

TOSHIE KANAYASU-TOYODA,¹ TAKAYOSHI SUZUKI,¹ TADASHI OSHIZAWA,¹ ERIKO UCHIDA,² TAKAO HAYAKAWA,² AND TERUhide YAMAGUCHI^{1*}

¹Division of Cellular and Gene Therapy Products, National Institute of Health Sciences, Tokyo, Japan

²National Institute of Health Sciences, Tokyo, Japan

Previously, we suggested that the phosphatidylinositol 3-kinase (PI3K)-p70 S6 kinase (p70 S6K) pathway plays an important role in granulocyte colony-stimulating factor (G-CSF)-dependent enhancement of the neutrophilic differentiation and proliferation of HL-60 cells. While atypical protein kinase C (PKC) has been reported to be a regulator of p70 S6K, abundant expression of PKC ζ was observed in myeloid and lymphoid cells. Therefore, we analyzed the participation of PKC ζ in G-CSF-dependent proliferation. The maximum stimulation of PKC ζ was observed from 15 to 30 min after the addition of G-CSF. From 5 to 15 min into this lag time, PKC ζ was found to translocate from the nucleus to the membrane. At 30 min it re-translocated to the cytosol. This dynamic translocation of PKC ζ was also observed in G-CSF-stimulated myeloperoxidase-positive cells differentiated from cord blood cells. Small interfering RNA for PKC ζ inhibited G-CSF-induced proliferation and the promotion of neutrophilic differentiation of HL-60 cells. These data indicate that the G-CSF-induced dynamic translocation and activation processes of PKC ζ are important to neutrophilic proliferation.

J. Cell. Physiol. 211: 189–196, 2006. © 2006 Wiley-Liss, Inc.

Hematopoietic cell differentiation is regulated by a complex network of growth and differentiation factors (Tenen et al., 1997; Ward et al., 2000). Granulocyte colony-stimulating factor (G-CSF) and its receptors are pivotal to the differentiation of myeloid precursors into mature granulocytes. In previous studies (Kanayasu-Toyoda et al., 2002) on the neutrophilic differentiation of HL-60 cells treated with either dimethyl sulfoxide (DMSO) or retinoic acid (RA), heterogeneous transferrin receptor (Trf-R) populations—transferrin receptor-positive (Trf-R⁺) cells and transferrin receptor-negative (Trf-R⁻) cells—appeared 2 days after the addition of DMSO or RA. The Trf-R⁺ cells were proliferative-type cells that had higher enzyme activity of phosphatidylinositol 3-kinase (PI3K) and protein 70 S6 kinase (p70 S6K), whereas the Trf-R⁻ cells were differentiation-type cells of which Tyr705 in STAT3 was much more phosphorylated by G-CSF. Inhibition of either PI3K by wortmannin or p70 S6K by rapamycin was found to eliminate the difference in differentiation and proliferation abilities between Trf-R⁺ and Trf-R⁻ cells in the presence of G-CSF (Kanayasu-Toyoda et al., 2002). From these results, we concluded that proteins PI3K and p70 S6K play important roles in the growth of HL-60 cells and negatively regulate neutrophilic differentiation. On the other hand, the maximum kinase activity of PI3K was observed at 5 min after the addition of G-CSF (Kanayasu-Toyoda et al., 2002) and that of p70 S6K was observed between 30 and 60 min after, indicating a lag time between PI3K and p70 S6K activation. It is conceivable that any signal molecule(s) must transduce the G-CSF signal during the time lag between PI3K and p70 S6K. Chung et al. (1994) also showed a lag time between PI3K and p70 S6K activation on HepG2 cells stimulated by platelet-derived growth factor (PDGF), suggesting that some signaling molecules also may transduce between PI3K and p70S6K.

Protein kinase C (PKC) is a family of Ser/Thr kinases involved in the signal transduction pathways that are triggered by numerous extracellular and intracellular stimuli. The PKC

family has been shown to play an essential role in cellular functions, including mitogenic signaling, cytoskeleton rearrangement, glucose metabolism, differentiation, and the regulation of cell survival and apoptosis. Eleven different members of the PKC family have been identified so far. Based on their structural similarities and cofactor requirements, they have been grouped into three subfamilies: (1) the classical or conventional PKCs (cPKC α , β_1 , β_2 , and γ), activated by Ca²⁺, diacylglycerol, and phosphatidyl-serine; (2) the novel PKCs (nPKC δ , ϵ , η , and θ), which are independent of Ca²⁺ but still responsive to diacylglycerol; and (3) the atypical PKCs (aPKC ζ and ι/λ), where PKC λ is the homologue of human PKC ζ . Atypical PKCs differ significantly from all other PKC family

Abbreviations: DMSO, dimethyl sulfoxide; MLPR, myeloid leukemia promyelocytic leukemia receptor; RA, retinoic acid; G-CSF, granulocyte colony-stimulating factor; Trf-R, transferrin receptor; BSA, bovine serum albumin; FITC, fluorescein isothiocyanate; PBS, phosphate-buffered saline; PKC, protein kinase C; PI3K, phosphatidylinositol 3-kinase; p70S6K, protein 70 S6 kinase; SDS-PAGE, sodium dodecyl sulfate-polyacrylamide gel electrophoresis; siRNA, small interfering RNA; PMN, polymorphonuclear leukocyte.

Contract grant sponsor: Ministry of Health, Labor, and Welfare of Japan.

Contract grant sponsor: Ministry of Education, Culture, Sports, Science, and Technology of Japan.

*Correspondence to: Teruhide Yamaguchi, Division of Cellular and Gene Therapy Products, National Institute of Health Sciences, 1-18-1, Kamiyoga, Setagaya-ku, Tokyo 158-8501, Japan.

E-mail: yamaguch@nihs.go.jp

Received 31 May 2006; Accepted 22 September 2006

Published online in Wiley InterScience (www.interscience.wiley.com.), 28 November 2006.

DOI: 10.1002/jcp.20930

members in their regulatory domains, in that they lack both the calcium-binding domain and one of the two zinc finger motifs required for diacylglycerol binding (Liu and Heckman, 1998). Romanelli et al. (1999) reported that p70 S6K is regulated by PKC ζ and participates in a PI3K-regulated signaling complex. On the other hand, Selbie et al. (1993) reported that the tissue distribution of PKC ζ is different from that of PKC ι/λ , and that PKC ι/λ appears to be widely expressed. If the p70 S6K could be activated by aPKC, the regulation of p70 S6K activation would seem to depend on the tissue-specific expression of PKC ι and/or PKC ζ . In neutrophilic lineage cells, the question is which aPKC participates in the regulation of p70 S6K on G-CSF signaling.

In this study, we show that G-CSF activated PKC ι , promoting its translocation from the nucleus to the cell surface membrane and subsequently to the cytosol in DMSO-treated HL-60 cells. We also show the translocation of PKC ι using myeloperoxidase-positive neutrophilic lineage differentiated from cord blood, which is a rich source of immature myeloid cells (Fritsch et al., 1993; Rappold et al., 1997; Huang et al., 1999; Debili et al., 2001; Hao et al., 2001). We concluded that PKC ι translocation and activation by G-CSF are needed for neutrophilic proliferation.

Materials and Methods

Reagents

Anti-p70 S6K polyclonal antibody was obtained from Santa Cruz Biotechnology (Santa Cruz, CA). Anti-PKC ι polyclonal antibody and monoclonal antibody were purchased from Santa Cruz Biotechnology and from Transduction Laboratories (Lexington, KY), respectively. Anti-PKC ζ polyclonal antibody was purchased from Cell Signaling Technology (Beverly, MA). Anti-myeloperoxidase antibody was purchased from Serotec Ltd. (Oxford, UK). GF 109203X, and Gö 6983 were obtained from Calbiochem-Novabiochem (San Diego, CA). Wortmannin was obtained from Sigma Chemical (St. Louis, MO). Anti-Histon-H1 antibody, anti-Fc γ receptor IIa (CD32) antibody, and anti-lactate dehydrogenase antibody were from Upstate Cell Signaling Solutions (Lake Placid, NY), Lab Vision Corp. (Fremont, CA), and Chemicon International, Inc. (Temecula, CA), respectively.

Cell culture

HL-60, Jurkut, K562, U937, and THP-1 cells were kindly supplied by the Japanese Collection of Research Bioresources Cell Bank (Osaka, Japan). Cells were maintained in RPMI 1640 medium containing 10% heat-inactivated FBS and 30 mg/L kanamycin sulfate at 37°C in moisturized air containing 5% CO $_2$. The HL-60 cells, which were at a density of 2.5×10^5 cells/ml, were differentiated by 1.25% DMSO. Two days after the addition of DMSO, the G-CSF-induced signal transduction was analyzed using either magnetically sorted cells or non-sorted cells.

Magnetic cell sorting

To prepare Trf-R $^-$ and Trf-R $^+$ cells, magnetic cell sorting was performed as previously reported (Kanayasu-Toyoda et al., 2002), using an automatic cell sorter (AUTO MACS; Miltenyi Biotec, Bergisch Gladbach, Germany). After cell sorting, both cell types were used for Western blotting and PKC ι enzyme activity analyses.

Preparation of cell lysates and immunoblotting

For analysis of PKC ι and PKC ζ expression, a PVDF membrane blotted with 50 μ g of various tissues per lane was purchased from BioChain Institute (Hayward, CA). Both a polymorphonuclear leukocytes (PMNs) fraction and a fraction containing lymphocytes and monocytes were isolated by centrifugation (400g, 25 min) using a Mono-poly resolving medium (Dai-Nippon Pharmaceutical, Osaka, Japan) from human whole blood, which was obtained from a healthy volunteer with informed consent. T-lymphocytes were further isolated from the mixture fraction using the Pan T Cell Isolation Kit (Miltenyi Biotec) according to the manufacturer's protocol. T-lymphocytes, PMNs, HL-60 cells, Jurkut cells, K562 cells, and U937 cells (1×10^7) were

collected and lysed in lysis buffer containing 1% Triton X-100, 10 mM K $_2$ HPO $_4$ /KH $_2$ PO $_4$ (pH 7.5), 1 mM EDTA, 5 mM EGTA, 10 mM MgCl $_2$, and 50 mM β -glycerophosphate, along with 1/100 (v/v) protease inhibitor cocktail (Sigma Chemical) and 1/100 (v/v) phosphatase inhibitor cocktail (Sigma Chemical). The cellular lysate of 10^6 cells per lane was subjected to Western blotting analysis. Human cord blood was kindly supplied from the Metro Tokyo Red Cross Cord Blood Bank (Tokyo, Japan) with informed consent. Mononuclear cells, isolated with the LymphoprepTM Tube (Axis-Shield PoC AS, Oslo, Norway), were cultured in RPMI 1640 medium containing 10% FBS in the presence of G-CSF for 3 days. Cultured cells were collected, and the cell lysate was subjected to Western blotting analysis.

A fraction of the plasma membrane, cytosol, and nucleus of the DMSO-treated HL-60 cells was prepared by differential centrifugation after the addition of G-CSF, as described previously (Yamaguchi et al., 1999). After the cells that had been suspended in 250 mM sucrose/10 mM Tris-HCl (pH 7.4) containing 1/100 (v/v) protease inhibitor cocktail (Sigma Chemical) were gently disrupted by freezing and thawing, they were centrifuged at 800g, 4°C for 10 min. The precipitation was suspended in 10 mM Tris-HCl (pH 6.7) supplemented with 1% SDS. It was then digested by benzonuclease at 4°C for 1 h and used as a sample of the nuclear fraction. After the post-nucleus supernatant was re-centrifuged at 100,000 rpm (452,000g) at a temperature of 4°C for 40 min, the precipitate was used as a crude membrane fraction and the supernatant as a cytosol fraction. Western blotting analysis was then performed as described previously (Kanayasu-Toyoda et al., 2002). The bands that appeared on x-ray films were scanned, and the density of each band was quantitated by Scion Image (Scion, Frederick, MD) using the data from three separate experiments.

Kinase assay

The activity of PKC ι was determined by phosphorous incorporation into the fluorescence-labeled pseudosubstrate (Pierce Biotechnology, Rockford, IL). The cell lysates were prepared as described above and immunoprecipitated with the anti-PKC ι antibody. Kinase activity was measured according to the manufacturer's protocol. In the analysis of inhibitors effects, cells were pretreated with a PI3K inhibitor, wortmannin (100 nM), or PKC inhibitors, GF109207X (10 μ M) and Gö6983 (10 μ M) for 30 min, and then stimulated by G-CSF for 15 min.

Observation of confocal laser-scanning microscopy

Upon the addition of G-CSF, PKC ι localization in the DMSO-treated HL-60 cells for 2 days was examined by confocal laser-activated microscopy (LSM 510, Carl Zeiss, Oberkochen, Germany). The cells were treated with 50 ng/ml G-CSF for the indicated periods and then fixed with an equal volume of 4.0% paraformaldehyde in PBS(-). After treatment with ethanol, the fixed cells were labeled with anti-PKC ι antibody and with secondary antibody conjugated with horseradish peroxidase. They were then visualized with TSATM Fluorescence Systems (PerkinElmer, Boston, MA).

Mononuclear cells prepared from cord blood cells were cultured in RPMI 1640 medium containing 10% FBS in the presence of G-CSF for 7 days. Then, for serum and G-CSF starvation, cells were cultured in RPMI 1640 medium containing 1% BSA for 11 h. After stimulation by 50 ng/ml G-CSF, the cells were fixed, stained with both anti-PKC ι polyclonal antibody and anti-myeloperoxidase monoclonal antibody, and finally visualized with rhodamine-conjugated anti-rabbit IgG and FITC-conjugated anti-mouse IgG, respectively.

RNA interference

Two pairs of siRNAs were chemically synthesized: annealed (Dharmacon RNA Technologies, Lafayette, CO) and transfected into HL-60 cells using NucleofectorTM (Amaxa, Cologne, Germany). The sequences of sense siRNAs were as follows: PKC ι , GAAGAAGCCUUUAGACUUUTA; p70 S6K, GCAAGGAGUCUAUCCAUGAUU. As a control, the sequence ACUCUAUCGCCAGCGUGACUU was used. Forty-eight hours after treatment with siRNA, the cells were lysed for Western blot analysis. For proliferation and differentiation assay, cells were transfected with siRNA on the first day, treated with DMSO on the second day, and supplemented with G-CSF on the third day. After cells were subsequently cultured for 5 days, cell numbers and formyl-Met-Leu-Phe receptor (fMLP-R) expression were determined.

fMLP-R expression

The differentiated cells were collected and incubated with FITC-conjugated fMLP; then, labeled cells were subjected to flow cytometric analysis (FACSCalibur, Becton Dickinson, Franklin Lakes, NJ).

Statistical analysis

Statistical analysis was performed using unpaired Student's *t*-test. Values of *P* < 0.05 were considered to indicate statistical significance. Each experiment was repeated at least three times and representative data were indicated.

Results**The distribution of atypical PKC in various tissues and cells**

Previously, we reported that the PI3K-p70 S6K-cMyc pathway plays an important role in the G-CSF-induced proliferation of DMSO-treated HL-60 cells, not only by enhancing the activity of both PI3K and p70 S6K but also by inducing the c-Myc protein (Kanayasu-Toyoda et al., 2002, 2003). We also reported that G-CSF did not stimulate Erk1, Erk2, or 4E-binding protein 1. The maximum kinase activity of PI3K was observed 5 min after the addition of G-CSF, and that of p70 S6K was observed between 30 and 60 min after. It is conceivable that any signal molecule(s) must transduce the G-CSF signal during the time lag between PI3K and p70 S6K. Romanelli et al. (1999) suggested that the activation of p70 S6K is regulated by PKC ζ and participates in the PI3K-regulated signaling complex. To examine the role of atypical PKC in the G-CSF-dependent activation and the relationship between atypical PKC and p70 S6K, the protein expression of PKC ζ and PKC ι in various human tissues and cells was analyzed by Western blotting. As shown in Figure 1A, both of the atypical PKCs were markedly expressed in lung and kidney but were weakly expressed in spleen, stomach, and placenta. In brain, cervix, and uterus, the expression of only PKC ι was observed. Selbie et al. (1993) have reported observing the expression of PKC ζ not in protein levels but in RNA levels, in the kidney, brain, lung, and testis, and that of PKC ι in the kidney, brain, and lung. In this study, the protein expression of PKC ι in the kidney, brain, and lung was consistent with the RNA expression of PKC ι . Despite the strong expression of PKC ζ RNA in brain (Selbie et al., 1993), PKC ζ protein was scarcely observed. Although PKC ι proteins were scarcely expressed in neutrophils and T-lymphocytes in peripheral blood, they were abundantly expressed in immature blood cell lines, that is, Jurkut, K562, U937, and HL-60 cells (Fig. 1B), in contrast with the very low expression of PKC ζ proteins. In mononuclear cells isolated from umbilical cord blood, which contains large numbers of immature myeloid cells and has a high proliferation ability, the expression of PKC ι proteins was also observed. Since Nguyen and Dessauer (2005) have reported observing abundant PKC ζ proteins in THP-1 cells, as a positive control for PKC ζ , we also performed a Western blot of THP-1 cells (Fig. 1B, right part). While PKC ι was markedly expressed in both THP-1 and HL-60 cells, PKC ζ was observed only in THP-1 cells. These data suggested that PKC ζ and PKC ι were distributed differently in various tissues and cells, and that mainly PKC ι proteins were expressed in proliferating blood cells.

Stimulation of PKC ι activity by G-CSF

Among the 11 different members of the PKC family, the α PKCs (ζ and ι) have been reported to activate p70 S6K activity and to be regulated by PI3K (Akimoto et al., 1998; Romanelli et al., 1999). As shown in Figure 1, although the PKC ζ proteins were not detected by Western blotting in HL-60 cells or mononuclear cells isolated from cord blood cells, it is possible that PKC ι could functionally regulate p70 S6K as an upstream

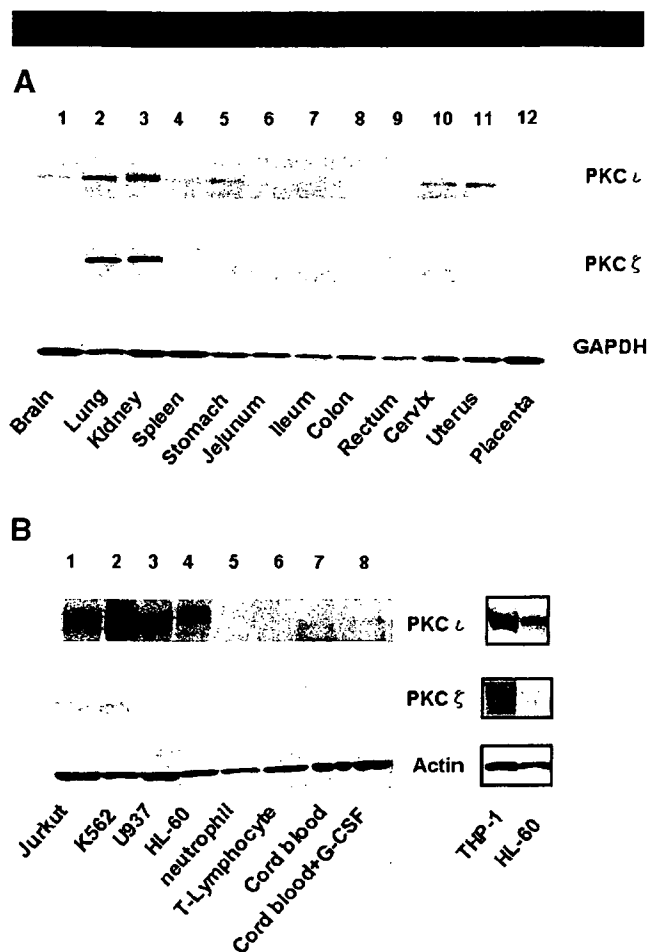


Fig. 1. Different distributions of PKC ζ and PKC ι . The protein expression of PKC ι appears in the upper part and that of PKC ζ in the middle part in various tissues and cells. A: 1, brain; 2, lung; 3, kidney; 4, spleen; 5, stomach; 6, jejunum; 7, ileum; 8, colon; 9, rectum; 10, cervix; 11, uterus; 12, placenta. Anti-GAPDH blot is a control for various tissues. B: 1, jurkut cells; 2, K562 cells; 3, U937 cells; 4, HL-60 cells; 5, neutrophils; 6, T-lymphocytes; 7, mononuclear cells from cord blood in the absence of G-CSF; 8, mononuclear cells from cord blood in the presence of G-CSF. Anti-actin blot is a control. The right part shows immunoblots of PKC ι , PKC ζ , and actin of THP-1 cells as a positive control for PKC ζ . The cell numbers of THP-1 and HL-60 cells were adjusted in relation to other cells on the left parts.

regulator in these cells. Therefore, we focused on the role of PKC ι as the possible upstream regulator of p70 S6K in neutrophil lineage cells. First, we compared the expression of PKC ι in both Trf-R $^{+}$ and Trf-R $^{-}$ cells. PKC ι proteins were expressed more abundantly in Trf-R $^{+}$ cells than in Trf-R $^{-}$ cells (Fig. 2A, middle part), as with the p70 S6K proteins. A time course study of PKC ι activity upon the addition of G-CSF revealed the maximum stimulation at 15 min, lasting until 30 min. The G-CSF-dependent activation of PKC ι was inhibited by the PKC inhibitors wortmannin, GF 109203X, and Gö 6983. Considering the marked inhibitory effect of wortmannin on PKC ι and evidence that the maximum stimulation of PI3K was observed at 5 min after the addition of G-CSF, PI3K was determined to be the upstream regulator of PKC ι in the G-CSF signal transduction of HL-60 cells. The basal activity of PKC ι in Trf-R $^{+}$ cells was higher than that in Trf-R $^{-}$ cells, and G-CSF was more augmented. In Trf-R $^{-}$ cells, PKC ι activity was scarcely stimulated by G-CSF. This tendency of PKC ι to be activated by G-CSF was similar to that of PI3K (Kanayasu-Toyoda et al., 2002).

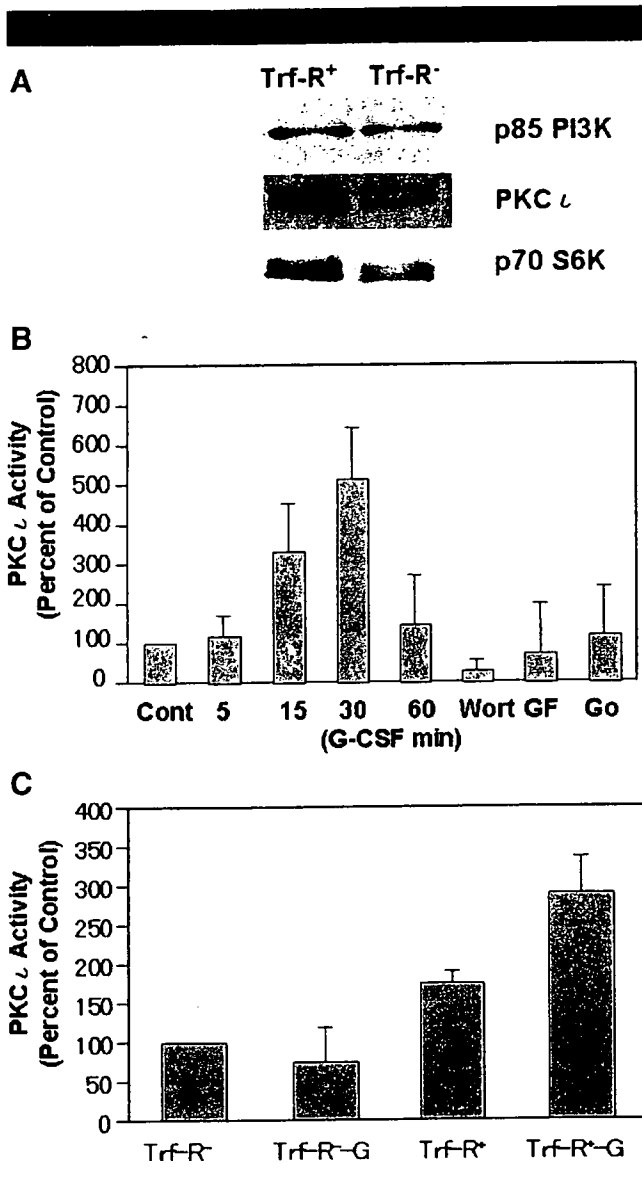


Fig. 2. Expression of PKC ι in Trf-R⁺ and Trf-R⁻ cells and effects of G-CSF on PKC ι activity. **A:** The expression of PKC ι in Trf-R⁺ and Trf-R⁻ cells was subjected to Western blot analysis after magnetic cell sorting. **B:** The G-CSF-dependent PKC ι activation of the DMSO-treated HL-60 cells was measured. The x-axis represents the time lapse (min) after the G-CSF stimulation and the y-axis percent of control that was not stimulated by G-CSF. Columns and bars represent the mean \pm SD, using data from three separate experiments. Wort: wortmannin (100 nM), GF: GF109207X (10 μ M), Gö: Gö6983 (10 μ M). Cells were pretreated with each inhibitor and then stimulated by G-CSF for 15 min. **C:** The PKC ι activity in the Trf-R⁺ and Trf-R⁻ cells 30 min after the addition of G-CSF. The y-axis represents the percentage of control that was non-stimulated Trf-R⁻ cells. Columns and bars represent the mean \pm SD, using data from three separate experiments.

Effects of G-CSF on PKC ι translocation

Muscella et al. (2003) demonstrated that the translocation of PKC ζ from the cytosol to the nucleus or membrane is required for c-Fos synthesis induced by angiotensin II in MCF-7 cells. It was also reported that high glucose induced the translocation of PKC ι (Chuang et al., 2003). These results suggest that the translocation of aPKC plays an important role in its signaling. To clarify the translocation of PKC ι , immuno-histochemical staining (Fig. 3) and biochemical fractionation (Fig. 4) in

DMSO-induced HL-60 cells were performed after the addition of G-CSF. In a non-stimulated condition, PKC ι in the HL-60 cells treated with DMSO for 2 days (Fig. 3, control) was detected mainly in the nucleus. Analysis of Western blotting (Fig. 4, left parts) and quantification of the bands (Fig. 4, right columns) also revealed that PKC ι was localized and observed mainly in the nuclear fraction (Fig. 4A). During the 5–15 min period after the addition of G-CSF, PKC ι was found to translocate (Figs. 3 and 4B) into the membrane fraction, after which it re-translocated into the cytosol fraction (Fig. 4C). In the presence of wortmannin, the G-CSF-induced translocation of PKC ι into the plasma membrane failed, but PKC ι was found to localize in the cytosolic fraction (Figs. 3 and 4B). Myeloperoxidase is thought to be expressed in stage from promyelocytes to mature neutrophils (Manz et al., 2002). In human cord blood cells (Fig. 3), PKC ι in the cells co-stained with anti-myeloperoxidase antibody was also localized in the nucleus after serum depletion (Fig. 3B top parts). Ten minutes after the addition of G-CSF, PKC ι was found to translocate into the membrane, and then into the cytosol at 30 min after the addition of G-CSF. In the presence of wortmannin, the G-CSF-induced translocation of PKC ι into the plasma membrane failed but PKC ι was found to localize in the cytosol. This suggested that the dynamic translocation of PKC ι induced by G-CSF is a universal phenomenon in neutrophilic lineage cells. Taken together, these data support the possibility that PI3K plays not only an important role upstream of PKC ι but also triggers the translocation from nucleus to membrane upon the addition of G-CSF.

In order to assess the purity of each cellular fraction, antibodies against specific markers were blotted. As specific markers, Histone H1, Fc γ receptor IIa (CD32), and lactate dehydrogenase (LDH) were used for the nuclear, membrane, and cytosolic fractions, respectively. The purities of the nuclear, membrane, and cytosolic fractions were 82.0, 78.5, and 72.2%, respectively (Fig. 4D).

Effects of siRNA for PKC ι on proliferation and differentiation

To determine the role of PKC ι in neutrophilic proliferation and differentiation, PKC ι was knocked down by siRNA. When the protein level of PKC ι was specifically downregulated by siRNA for PKC ι (Fig. 5A), G-CSF failed to enhance proliferation of the cells during 5 days' cultivation (Fig. 5B). The effect of siRNA for PKC ι on neutrophilic differentiation in terms of fMLP-R expression was also determined. As shown in Figure 5C, fMLP-R expression was promoted by siRNA for PKC ι in either the presence (lower part) or absence (upper part) of G-CSF. These data indicate that PKC ι positively regulates G-CSF-induced proliferation and negatively regulates the differentiation of DMSO-treated HL-60 cells.

Discussion

We previously reported that PI3K/p70 S6K plays an important role in the regulation of the neutrophilic differentiation and proliferation of HL-60 cells. Akimoto et al. (1998) and Romanelli et al. (1999) reported that p70 S6K is regulated by aPKC and aPKC λ /PKC ζ , respectively. At first, we showed that the distribution of PKC ζ and PKC ι proteins in various human tissues and cells was not similar (Fig. 1A), and that PKC ι are more abundantly expressed in proliferating blood cells: Jurkat, K562, U937, and HL-60 cells (Fig. 1B). Moreover, PKC ι proteins were also observed in cultured mononuclear cells of cord blood, in which the myeloid progenitors were enriched in the presence or absence of G-CSF (Fig. 1B). The myeloperoxidase-positive cells as neutrophilic lineage cells, a myeloid marker, were also stained with the antibody of PKC ι (Fig. 3B). Although PKC ζ proteins are barely detected in

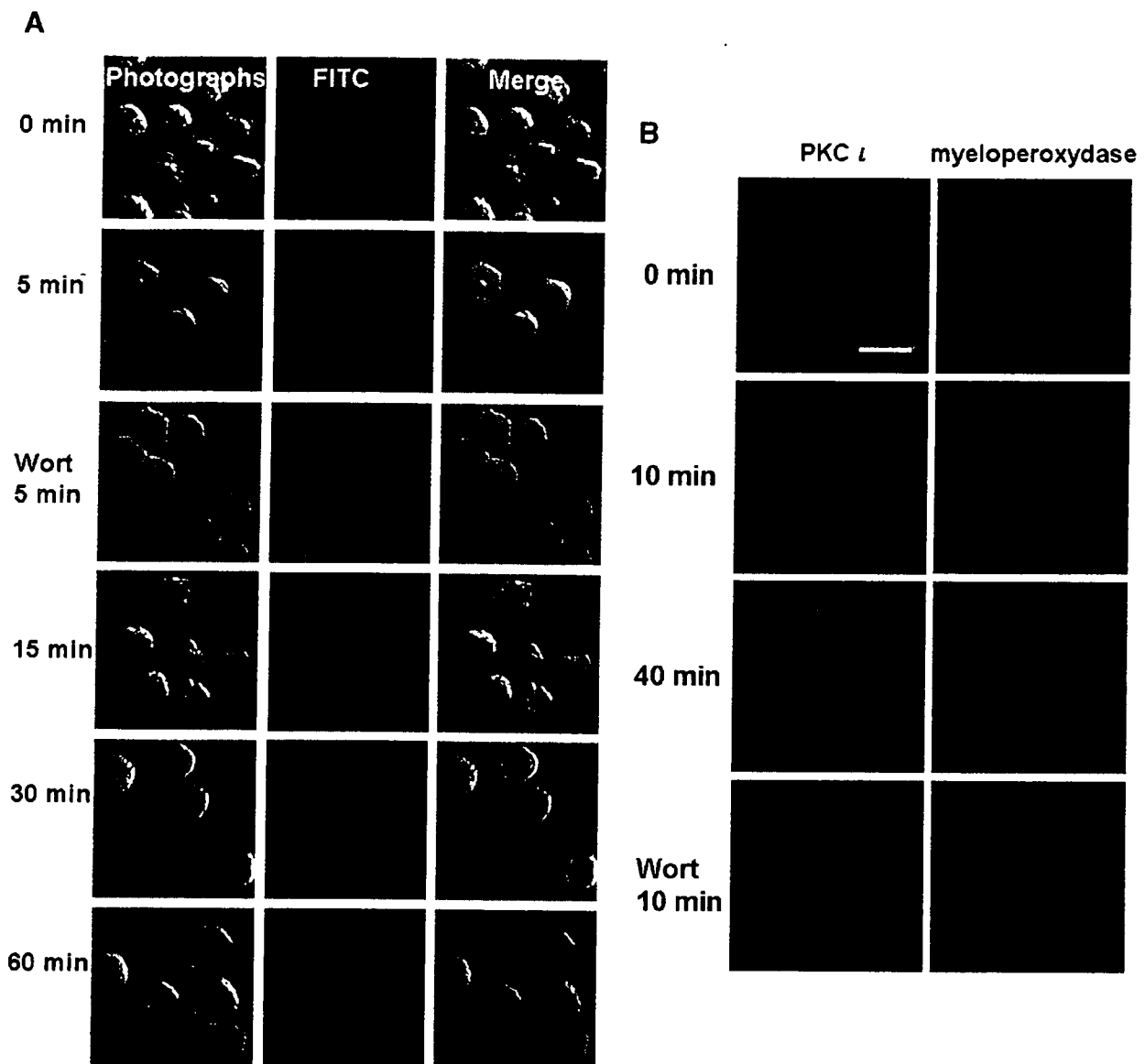


Fig. 3. Translocation of PKC ζ after the activation of G-CSF. **A:** 2 days after the addition of DMSO, HL-60 cells stimulated by G-CSF were fixed, incubated with anti-PKC ζ antibody, and visualized as described above. The photographs can be seen at the left part of the figure, the fluorescent photographs in the middle of the figure, and the merged images at the right. **B:** G-CSF-stimulated mononuclear cells from cord blood were stained with anti-PKC ζ antibody (red, left part) and anti-myeloperoxidase antibody (green, right part) after serum depletion. Under no stimulation, PKC ζ was observed in the nucleus. G-CSF promoted the translocation of PKC ζ to the membrane within 5–15 min, and then to the cytosol. Wort: wortmannin. White bar: 10 μ m.

neutrophilic HL-60 cells, PKC ζ proteins were markedly expressed in these cells (Fig. 1B). This study showed, for the first time, the stimulation of PKC ζ activity in G-CSF-treated HL-60 cells (Fig. 2B) at 15–30 min after the addition of G-CSF. Maximum activation from the addition of NGF in PC12 cells was also observed at 15 min (Wooten et al., 2001). Atypical PKCs are lipid-regulated kinases that need to be localized to the membrane in order to be activated. PKC ζ is directly activated by phosphatidylinositol 3,4,5-trisphosphate, a product of PI3K (Nakanishi et al., 1993). We previously reported that the maximum activation of PI3K was observed in HL-60 cells 5 min after the addition of G-CSF (Kanayasu-Toyoda et al., 2002). Most investigators have reported the translocation of aPKC in either muscle cells or adipocytes stimulated by insulin (Andjelkovic et al., 1997; Goransson et al.,

1998; Galetic et al., 1999; Standaert et al., 1999; Braiman et al., 2001; Chen et al., 2003; Kanzaki et al., 2004; Sasaoka et al., 2004; Herr et al., 2005). In response to insulin stimulation, aPKC ζ/λ is translocated to the plasma membrane (Standaert et al., 1999; Braiman et al., 2001), where aPKC ζ/λ is believed to be activated (Galetic et al., 1999; Kanzaki et al., 2004). In the present study, the addition of G-CSF induced PKC ζ to translocate to the membrane from the nucleus within 5–15 min (Figs. 3 and 4), and this translocation to the plasma membrane accompanied the full activation of PKC ζ (Fig. 2B). Previously we reported also that the maximum activation of p70 S6K in HL-60 cells was observed from 30 to 60 min after the addition of G-CSF (Kanayasu-Toyoda et al., 1999, 2002), suggesting that there was a time lag between the activation of PI3K and p70 S6K upon the addition of G-CSF in HL-60 cells. In the present study, PKC ζ was

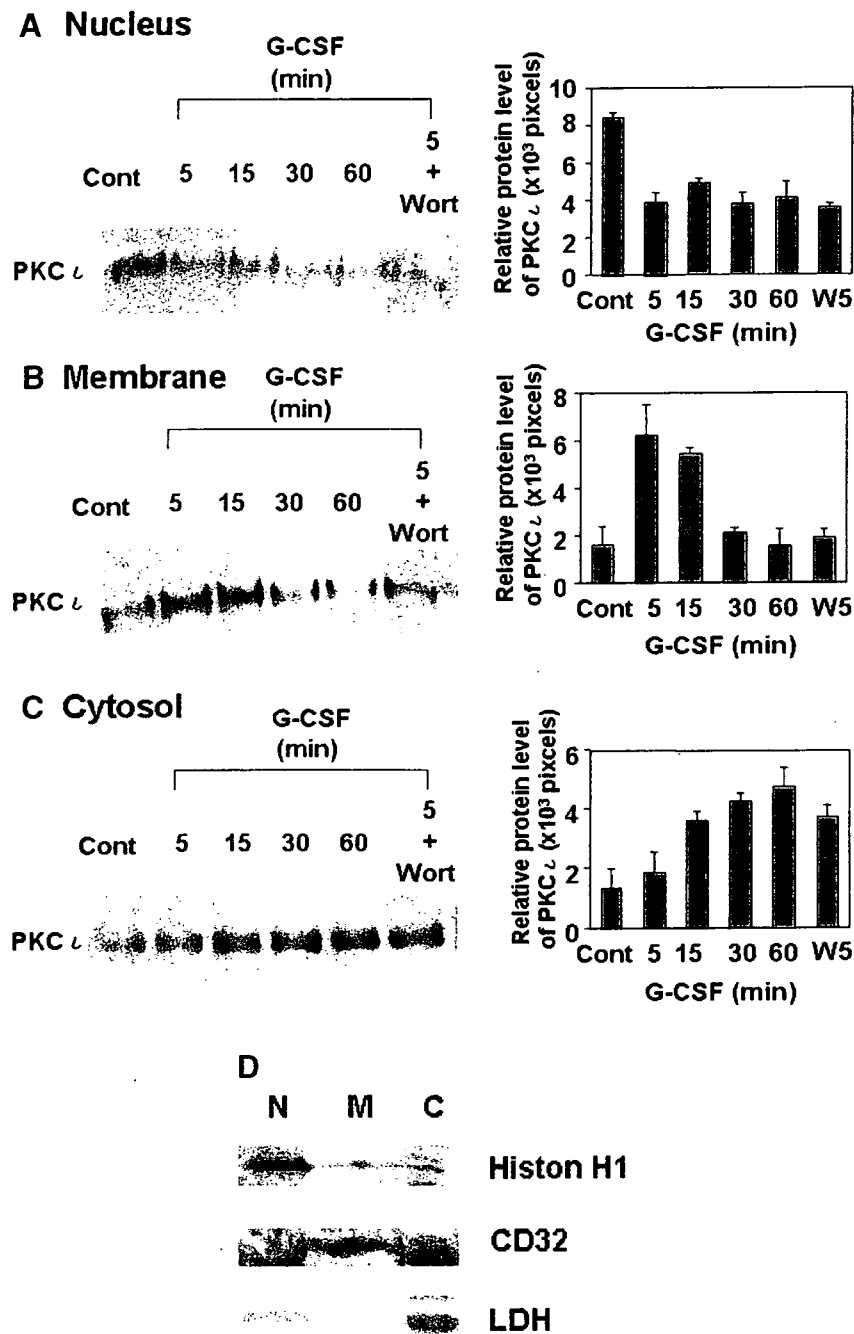


Fig. 4. Translocation of PKC ζ after activation by G-CSF on biochemical fractionation. The cells were differentiated as described in the Figure 3 legend. After stimulation by G-CSF, the amounts of PKC ζ proteins in the nucleus (A), plasma membrane (B), and cytosol (C), as fractionated by differential centrifugation, were analyzed by Western blotting (left parts). The right parts show the quantitation of the bands of PKC ζ proteins. Wort or W: wortmannin. PKC ζ protein was quantitated using data from three separate experiments. Columns and bars represent the mean \pm SD. D: Each cell fraction was immunoblotted with antibodies of specific marker. Histon-H1, Fc γ receptor IIa (CD32), and lactate dehydrogenase (LDH) are specific markers for nuclear (N), membrane (M), and cytosolic (C) fractions, respectively.

found to re-translocate from the plasma membrane to the cytosol (Figs. 3 and 4C). In the presence of wortmannin, an inhibitor of PI3K, PKC ζ failed to translocate into the plasma membrane, but instead translocated to cytosol directly from the nucleus upon the addition of G-CSF (Figs. 3 and 4B). PKC ζ translocation was also observed in myeloperoxidase-positive cells derived from human cord blood (Fig. 3B), indicating that G-CSF-induced dynamic translocation of PKC ζ occurred in not

only a limited cell line but also neutrophilic lineage cells. These data suggest that PI3K plays an important role in the activation and translocation of PKC ζ during the G-CSF-induced activation of myeloid cells. Furthermore, the translocation to the plasma membrane in response to G-CSF is wortmannin sensitive, but the translocation from the nucleus upon G-CSF stimulation is not affected by wortmannin, suggesting that the initial signal of G-CSF-induced PKC ζ translocation from the nucleus may be

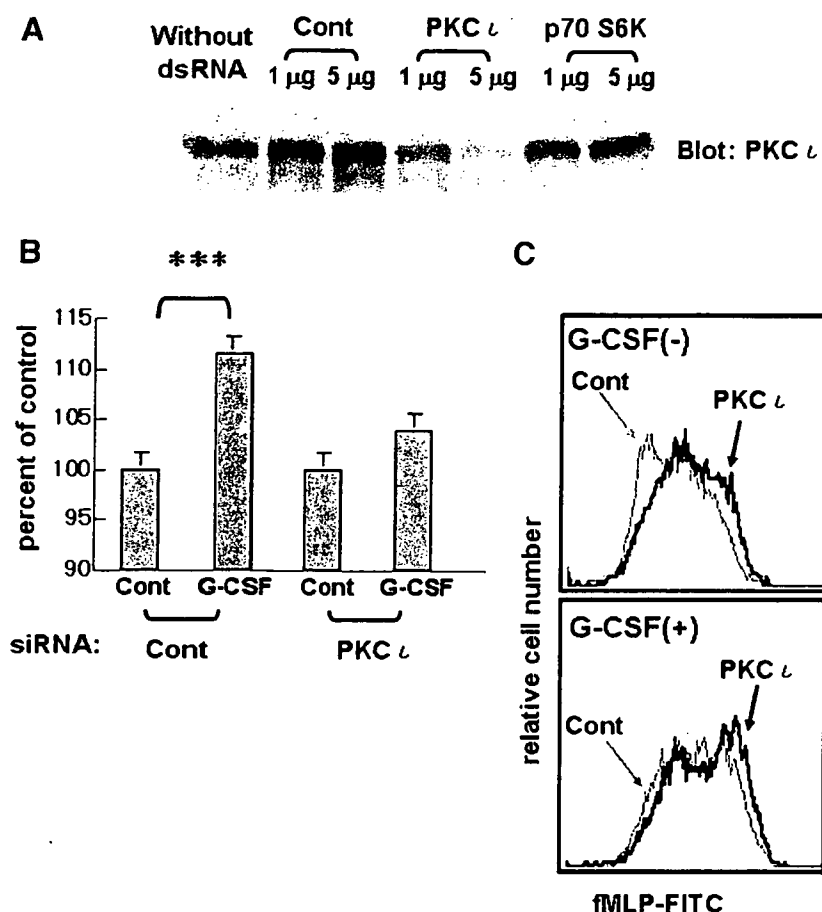


Fig. 5. Effects of siRNA of PKC ζ on proliferation, differentiation, and phosphorylation at various sites of p70 S6K. **A:** Forty-eight hours after transfection with siRNA of PKC ζ or p70 S6K, protein levels of PKC ζ were compared. **B:** Proliferation of the cells transfected with siRNA of PKC ζ or control (Cont) was measured 5 days after the addition of G-CSF. Columns and bars represent the mean \pm SD of triplicate wells (***) $P < 0.001$). **C:** fMLP-R expression was analyzed by flow cytometry 5 days after the addition of G-CSF. The gray arrow indicates cells transfected with the control sequence of double-stranded RNA (Cont, gray lines), and the black arrow the cells transfected with siRNA for PKC ζ (black lines) in the presence (lower part) or absence (upper part) of G-CSF.

PI3K-independent, but association of PKC ζ with the plasma membrane could be mediated through a PI3K-dependent signal. Cord blood is an important material of blood transplantation for leukemia (Bradstock et al., 2006; Ooi, 2006; Yamada et al., 2006) or for congenital neutropenia (Mino et al., 2004; Nakazawa et al., 2004) because it contains many hematopoietic stem cells such as CD34-positive cells or CD133-positive cells, and also contains immature granulocytes. The neutrophilic differentiation and proliferation are necessary processes after transplantation.

Formyl-Met-Leu-Phe peptide evokes the migration, superoxide production, and phagocytosis of neutrophils through fMLP-R, a suitable marker for neutrophilic differentiation. In this study, the reduction of PKC ζ by siRNA inhibited G-CSF-induced proliferation (Fig. 5B) and promoted neutrophilic differentiation (Fig. 5C) in terms of fMLP-R expression. These data, however, suggest that PKC ζ promoted G-CSF-induced proliferation and blocked differentiation at the same time.

The substrates of aPKC have recently been reported: namely, the cytoskeletal protein Lethal giant larvae (Lgl) was phosphorylated by *Drosophila* aPKC (Betschinger et al., 2003) and glyceraldehydes-3-phosphate dehydrogenase (GAPDH) was phosphorylated by PKC ζ (Tisdale, 2002) directly in both cases. While the direct phosphorylation of p70 S6K by aPKC was not observed (Akimoto et al., 1998; Romanelli et al.,

1999), the enzyme activity of p70 S6K was markedly enhanced by co-transfection with aPKC and PDK-1, the latter of which is recruited to the membrane due to the binding of phosphatidylinositol-3,4,5-trisphosphate to its PH domain (Anderson et al., 1998). The addition of G-CSF induced PKC ζ to increase phosphorylation at Thr-389, which is the site most closely related to enzyme activity among the multi-phosphorylation sites of p70 S6K (Weng et al., 1998). However, the mammalian target of rapamycin (mTOR), an upstream regulator, also phosphorylates Thr-389 of p70 S6K and markedly stimulates p70 S6K activity under coexistence with PDK-1 (Isotani et al., 1999). We could not rule out the possibility that other PKC isoforms can contribute to the activation of p70 S6K. We postulated that in G-CSF-stimulated HL-60 cells, PKC ζ contributes to p70 S6K activation as an upstream regulator.

Atypical PKC isoforms are reported to play an important role in the activation of I κ B kinase β (Lallena et al., 1999). In PKC ζ -deficient mice, impaired signaling through the B-cell receptor resulted in the inhibition of cell proliferation and survival while also causing defects in the activation of ERK and the transcription of NF- κ B-dependent genes (Martin et al., 2002). Moreover, Lafuente et al. (2003) demonstrated that the loss of Par-4, that is, the genetic inactivation of the aPKC inhibitor, led to an increased proliferative response of

peripheral T cells when challenged through the T-cell receptor. However, it has been reported that PKC λ -deficient mice have a lethal phenotype at the early embryonic stage (Soloff et al., 2004). Based on the present results and those of previous reports (Kanayasu-Toyoda et al., 1999, 2002), we postulate that PKC ι plays an important role in regulating G-CSF-induced proliferation in neutrophilic lineage cells.

Acknowledgments

We thank the Metro Tokyo Red Cross Cord Blood Bank (Tokyo, Japan) for their kind cooperation. This work was supported in part by a grand-in-aid for health and labor science research (H17-SAISEI-021) from the Japanese Ministry of Health, Labor and Welfare, and in part by a grand-in-aid for Research on Health Sciences focusing on Drug Innovation from the Japan Health Sciences Foundation.

Literature Cited

- Akimoto K, Nakaya M, Yamanaka T, Tanaka J, Matsuda S, Weng QP, Avruch J, Ohno S. 1998. Atypical protein kinase C λ binds and regulates p70 S6 kinase. *Biochem J* 335:417–424.
- Anderson KE, Coadwell J, Stephens LR, Hawkins PT. 1998. Translocation of PDK-1 to the plasma membrane is important in allowing PDK-1 to activate protein kinase B. *Curr Biol* 8:684–691.
- Andjelkovic M, Alessi DR, Meier R, Fernandez A, Lamb NJ, Frech M, Cron P, Cohen P, Lucocq JM, Hemmings BA. 1997. Role of translocation in the activation and function of protein kinase B. *J Biol Chem* 272:31515–31524.
- Betschinger J, Mechtler K, Knoblich JA. 2003. The Par complex directs asymmetric cell division by phosphorylating the cytoskeletal protein Lgl. *Nature* 422:326–330.
- Bradstock KF, Hertzberg MS, Kerridge IH, Svernilson J, McGurgan M, Huang G, Antonenas V, Gottlieb DJ. 2006. Unrelated umbilical cord blood transplantation for adults with haematological malignancies: Results from a single Australian centre. *Intern Med J* 36:355–361.
- Braiman L, Alt A, Kuroki T, Ohba M, Bak A, Tennenbaum T, Sampson SR. 2001. Activation of protein kinase C zeta induces serine phosphorylation of VAMP2 in the GLUT4 compartment and increases glucose transport in skeletal muscle. *Mol Cell Biol* 21:7852–7861.
- Chen X, Al-Hasani H, Olausson T, Wentzhel AM, Smith U, Cushman SW. 2003. Activity, phosphorylation state and subcellular distribution of GLUT4-targeted Akt2 in rat adipose cells. *J Cell Sci* 116:3511–3518.
- Chuang LY, Guh JY, Liu SF, Hung MY, Liao TN, Chiang TA, Huang JS, Huang YL, Lin CF, Yang YL. 2003. Regulation of type II transforming-growth-factor-beta receptors by protein kinase C ι . *Biochem J* 375:385–393.
- Chung J, Grammer TC, Lemon KP, Kazlauskas A, Blenis J. 1994. PDGF- and insulin-dependent p70 S6K activation mediated by phosphatidylinositol-3-OH kinase. *Nature* 370:71–75.
- Debili N, Robin C, Schiavon V, Letestu R, Pflumio F, Mitjavila-Garcia MT, Coulombel L, Vainchenker W. 2001. Different expression of CD41 on human lymphoid and myeloid progenitors from adults and neonates. *Blood* 97:2023–2030.
- Fritsch G, Buchinger P, Printz D, Fink FM, Mann G, Peters C, Wagner T, Adler A, Gadner H. 1993. Rapid discrimination of early CD34+ myeloid progenitors using CD45-RA analysis. *Blood* 81:2301–2309.
- Galetic I, Andjelkovic M, Meier R, Brodbeck D, Park J, Hemmings BA. 1999. Mechanism of protein kinase B activation by insulin/insulin-like growth factor-1 revealed by specific inhibitors of phosphoinositide 3-kinase—Significance for diabetes and cancer. *Pharmacol Ther* 82:409–425.
- Goransson O, Wijkander J, Manganiello V, Degerman E. 1998. Insulin-induced translocation of protein kinase B to the plasma membrane in rat adipocytes. *Biochem Biophys Res Commun* 246:249–254.
- Hao QL, Zhu J, Price MA, Payne KJ, Barsky LW, Crooks GM. 2001. Identification of a novel, human multilineage progenitor in cord blood. *Blood* 97:3683–3690.
- Herr HJ, Bernard JR, Reeder DW, Rivas DA, Limon JJ, Yaspelkis BB3rd. 2005. Insulin-stimulated plasma membrane association and activation of Akt2, aPKC zeta and aPKC lambda in high fat fed rodent skeletal muscle. *J Physiol* 565:627–636.
- Huang S, Chen Z, Yu JF, Young D, Bashay A, Ho AD, Law P. 1999. Correlation between IL-3 receptor expression and growth potential of human CD34+ hematopoietic cells from different tissues. *Stem Cells* 17:265–272.
- Isotani S, Hara K, Tokunaga C, Inoue H, Avruch J, Yonezawa K. 1999. Immunopurified mammalian target of rapamycin phosphorylates and activates p70 S6 kinase alpha in vitro. *J Biol Chem* 274:34493–34498.
- Kanayasu-Toyoda T, Yamaguchi T, Uchida E, Hayakawa T. 1999. Commitment of neutrophilic differentiation and proliferation of HL-60 cells coincides with expression of transferrin receptor. Effect of granulocyte colony stimulating factor on differentiation and proliferation. *J Biol Chem* 274:25471–25480.
- Kanayasu-Toyoda T, Yamaguchi T, Oshizawa T, Kogi M, Uchida E, Hayakawa T. 2002. Role of the p70 S6 kinase cascade in neutrophilic differentiation and proliferation of HL-60 cells—a study of transferrin receptor-positive and -negative cells obtained from dimethyl sulfoxide- or retinoic acid-treated HL-60 cells. *Arch Biochem Biophys* 405:21–31.
- Kanayasu-Toyoda T, Yamaguchi T, Oshizawa T, Uchida E, Hayakawa T. 2003. The role of c-Myc on granulocyte colony-stimulating factor-dependent neutrophilic proliferation and differentiation of HL-60 cells. *Biochem Pharmacol* 66:133–140.
- Kanzaki M, Mora S, Hwang JB, Saltiel AR, Pessin JE. 2004. Atypical protein kinase C (PKCzeta/lambda) is a convergent downstream target of the insulin-stimulated phosphatidylinositol 3-kinase and TC10 signaling pathways. *J Cell Biol* 164:279–290.
- Lafuente MJ, Martin P, Garcia-Cao I, Diaz-Meco MT, Serrano M, Moscat J. 2003. Regulation of mature T lymphocyte proliferation and differentiation by Par-4. *Embo J* 22:4689–4698.
- Lallena MJ, Diaz-Meco MT, Bren G, Paya CV, Moscat J. 1999. Activation of IkappaB kinase beta by protein kinase C isoforms. *Mol Cell Biol* 19:2180–2188.
- Liu WS, Heckman CA. 1998. The sevenfold way of PKC regulation. *Cell Signal* 10:529–542.
- Manz MG, Miyamoto T, Akashi K, Weissman IL. 2002. Prospective isolation of human clonogenic common myeloid progenitors. *Proc Natl Acad Sci USA* 99:11872–11877.
- Martin P, Duran A, Minguet S, Gaspar ML, Diaz-Meco MT, Rennert P, Leitges M, Moscat J. 2002. Role of zeta PKC in B-cell signaling and function. *Embo J* 21:4049–4057.
- Mino E, Kobayashi R, Yoshida M, Suzuki Y, Yamada M, Kobayashi K. 2004. Umbilical cord blood stem cell transplantation from unrelated HLA-matched donor in an infant with severe congenital neutropenia. *Bone Marrow Transplant* 33:969–971.
- Muscella A, Greco S, Elia MG, Storelli C, Marsigliante S. 2003. PKC-zeta is required for angiotensin II-induced activation of ERK and synthesis of C-FOS in MCF-7 cells. *J Cell Physiol* 197:61–68.
- Nakanishi H, Brewer KA, Exton JH. 1993. Activation of the zeta isozyme of protein kinase C by phosphatidylinositol 3,4,5-trisphosphate. *J Biol Chem* 268:13–16.
- Nakazawa Y, Sakashita K, Kinoshita M, Saida K, Shigemura T, Yanagisawa R, Shikama N, Kamijo T, Koike K. 2004. Successful unrelated cord blood transplantation using a reduced-intensity conditioning regimen in a 6-month-old infant with congenital neutropenia complicated by severe pneumonia. *Int J Hematol* 80:287–290.
- Nguyen BT, Dessauer CW. 2005. Relaxin stimulates protein kinase C zeta translocation: Requirement for cyclic adenosine 3',5'-monophosphate production. *Mol Endocrinol* 19:1012–1023.
- Ooi J. 2006. The efficacy of unrelated cord blood transplantation for adult myelodysplastic syndrome. *Leuk Lymphoma* 47:599–602.
- Rappold I, Ziegler BL, Kohler I, Marchetto S, Rosnet O, Birnbaum D, Simmons PJ, Zannettino AC, Hill B, Neu S, Knapp W, Alitalo R, Alitalo K, Ullrich A, Kanz L, Bühring HJ. 1997. Functional and phenotypic characterization of cord blood and bone marrow subsets expressing FLT3 (CD135) receptor tyrosine kinase. *Blood* 90:111–125.
- Romanelli A, Martin KA, Toker A, Blenis J. 1999. p70 S6 kinase is regulated by protein kinase C ζ and participates in a phosphoinositide 3-kinase-regulated signalling complex. *Mol Cell Biol* 19:2921–2928.
- Sasaoka T, Wada T, Fukui K, Murakami S, Ishihara H, Suzuki R, Tobe K, Kadowaki T, Kobayashi M. 2004. SH2-containing inositol phosphatase 2 predominantly regulates Akt2, and not Akt1, phosphorylation at the plasma membrane in response to insulin in 3T3-L1 adipocytes. *J Biol Chem* 279:14835–14843.
- Selbie LA, Schmitz-Peiffer C, Sheng Y, Biden TJ. 1993. Molecular cloning and characterization of PKC ι , an atypical isoform of protein kinase C derived from insulin-secreting cells. *J Biol Chem* 268:24296–24302.
- Soloff RS, Katayama C, Lin MY, Feramisco JR, Hedrick SM. 2004. Targeted deletion of protein kinase C lambda reveals a distribution of functions between the two atypical protein kinase C isoforms. *J Immunol* 173:3250–3260.
- Standaert ML, Bandyopadhyay G, Perez L, Price D, Galloway L, Poklepovic A, Sajan MP, Cenni V, Sirri A, Moscat J, Toker A, Farese RV. 1999. Insulin activates protein kinases C-zeta and C-lambda by an autophosphorylation-dependent mechanism and stimulates their translocation to GLUT4 vesicles and other membrane fractions in rat adipocytes. *J Biol Chem* 274:25308–25316.
- Tenen DG, Hromas R, Licht JD, Zhang DE. 1997. Transcription factors, normal myeloid development, and leukemia. *Blood* 90:489–519.
- Tisdale EJ. 2002. Glyceroldehyde-3-phosphate dehydrogenase is phosphorylated by protein kinase C ι /lambda and plays a role in microtubule dynamics in the early secretory pathway. *J Biol Chem* 277:3334–3341.
- Ward AC, Loeb DM, Soede-Bobok AA, Touw IP, Friedman AD. 2000. Regulation of granulopoiesis by transcription factors and cytokine signals. *Leukemia* 14:973–990.
- Weng QP, Kozlowski M, Belham C, Zhang A, Comb MJ, Avruch J. 1998. Regulation of the p70 S6 kinase by phosphorylation in vivo. Analysis using site-specific anti-phosphopeptide antibodies. *J Biol Chem* 273:16621–16629.
- Wooten MW, Vandenplas ML, Seibenhener ML, Geetha T, Diaz-Meco MT. 2001. Nerve growth factor stimulates multisite tyrosine phosphorylation and activation of the atypical protein kinase C's via a src kinase pathway. *Mol Cell Biol* 21:8414–8427.
- Yamada K, Mizusawa M, Harima A, Kajiwara K, Hamaki T, Hoshi K, Kozai Y, Kodo H. 2006. Induction of remission of relapsed acute myeloid leukemia after unrelated donor cord blood transplantation by concomitant low-dose cytarabine and calcitriol in adults. *Eur J Haematol* 77:345–348.
- Yamaguchi T, Mukasa T, Uchida E, Kanayasu-Toyoda T, Hayakawa T. 1999. The role of STAT3 in granulocyte colony-stimulating factor-induced enhancement of neutrophilic differentiation of Me2SO-treated HL-60 cells. GM-CSF inhibits the nuclear translocation of tyrosine-phosphorylated STAT3. *J Biol Chem* 274:15575–15581.

JCRB 細胞バンク：厚生労働省

小原有弘、水澤 博〔独立行政法人 医薬基盤研究所 生物資源研究部 細胞資源研究室 (JCRB 細胞バンク)〕

機関名：独立行政法人 医薬基盤研究所 生物資源研究部 細胞資源研究室 (JCRB 細胞バンク)

URL：http://cellbank.nibio.go.jp/

I. リソースの特徴

培養細胞は生命科学研究にとって必要不可欠な研究資源として十分に認識されており、非常に広範な研究に利用されるリソースとなっている。細胞は生物の最も基本的な構成単位であり、生命現象を再現できる最小単位が細胞であると言える。細胞は培養条件を制御することにより増殖させたり、機能を持った細胞へ分化させることも可能である。細胞を用いた研究は多岐に渡っているが大きく3つの研究に分けられる。第1に培養細胞を生体の模倣として使用し、培養細胞内で起こる事象を解析することで、生体内で起こっていることをより詳しく解明する研究。第2に遺伝子導入や遺伝子ノックアウトなど生体内とは異なる環境・状況を培養細胞で構築し、その解析を行うことで作り出した環境・状況が生体に与える影響を考える研究。第3に培養細胞を抗体産生や生理活性物質生産などのツールとして使用する研究。これら3つの研究において細胞が万能であるとは言えないが非常に有用な研究資源と言える。以前はよく増殖し、広く頒布しやすい癌細胞などの株化細胞が研究に広く

利用されていたが、近年はヒトへの医療応用や治療法開発に向けて、機能や分化能をある程度維持したヒト由来の正常細胞や遺伝子導入細胞、不死化細胞の研究利用ニーズが高く、新たな研究資源の開発も進んでいる。

II. リソースの整備状況

JCRB細胞バンクは1985年、厚生労働省（当時の厚生省）によって我が国初の細胞バンクとして設立され、生命科学研究全体の発展とともに細胞バンク事業も発展してきた。現在の登録細胞数は1,018種類（2007年6月）で、主にヒト由来細胞（622種類、61%）がコレクションされ厚生労働行政に資する研究に利用されている。また、2007年より京都大学放射線生物研究センターで収集された高発癌性遺伝病患者由来細胞1,999株（表1）の分譲を開始した。JCRB細胞バンクでは高品質な細胞提供を行っており、マイコプラズマなどの微生物汚染検査、細胞のクロスコンタミネーション（細胞の入れ替わり）などを検査する細胞個別識別検査、染色体解析、性状検査などの品質管理を実施し、ガラスアンプルに細胞を封入した状態で液体窒素保存容器に保管した

表1. 高発癌性遺伝病患者由来細胞コレクション

疾患名	株数	疾患名	株数	疾患名	株数
網膜芽細胞腫	651	家族性白血病	23	甲状腺髄様癌	5
色素性乾皮症	411	ブルーム症候群	20	色素失調症	4
ファンconi貧血	232	ポイツ・イエーガー症候群	19	色素異常症	4
再生不良性貧血	124	疣贅状表皮発育異常症	14	基底細胞母斑症候群	4
コケイン症候群	83	シップル症候群	13	肝芽腫	4
毛細血管拡張性運動失調症	82	ダウン症候群	12	バックウイズ・ウィーデマン症候群	4
家族性大腸ポリポーシス	71	ロスモンド・トムソン症候群	9	その他	159
先天性異常・先天性奇形	43	ガードナー症候群	8		

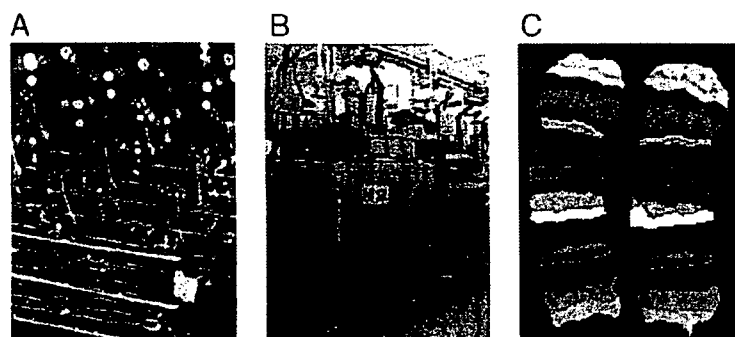


図1. JCRB 細胞バンクでの細胞品質に関わる取り組み

A：高品質な細胞アンプル。

B：超低温（液体窒素）細胞凍結保存容器。

C：mBand法による染色体詳細解析。

細胞を分譲している。年間に分譲するアンブル数は3,000を超えて年々増加する傾向にあり、2006年度は3,529アンブルであった。また、リソースを海外に分譲する体制も十分に確立しており、年間250アンブル程度を欧米を中心に分譲しているが、近年はアジア諸国への分譲も増加している。

Ⅲ. 国際連携

海外ではATCC (American Type Culture Collection) や ECACC (European Collection of Animal Cell Cultures) に代表される細胞バンクが点在しており、非常に多くの細胞を保有している。海外のバンクとはJCRB細胞バンク設立当初より緊密に情報交換を行っており、クロスカルチャーコンタミネーションのデータは共通利用できるフォーマットを用いて連携して情報提供を行っている。また、The Society for In Vitro Biology においては細胞バンク委員会が設置され、品質管理方法の標準化や標準株の基準などに関して議論が進められている。その他国際共同研究としてHeLa細胞のクロスコンタミネーション状況に関する調査を実施し報告を行い、経済協力開発機構 (Organization for Economic Co-operation and Development; OECD) においては連携してガイドライン (Human Derived Material Best Practice) を制定するべく活動し、国際連携が積極的に行われている。

Ⅳ. 細胞資源の品質に関する調査と研究例

1. マイコプラズマによる細胞の汚染

マイコプラズマは自己増殖能を持つ細菌の1/10程度の大きさの微生物であり、培養細胞と共存して増殖するが、汚染しても培地が濁ったりしないので混入に気づきにくい。汚染した細胞のタンパク質の25%、DNAの25%程度はマイコプラズマ由来のものと考えられ、細胞の増殖や遺伝子発現など多くの細胞機能に影響を与えることが報告されている。2007年に簡易検査法 (Cambrex社製, MycoAlert™) による全国調査を行った結果、900検体中197検体 (約22%) において陽性判定となり、研究室で使われている細胞の汚染が深刻な問題となっていることが明らかとなった。

2. STR (short tandem repeat) 解析によるヒト由来細胞個別識別

STR解析はゲノム中に存在する2~数個の塩基から成る繰り返し配列 [(CAG)_n、(GC)_n など] の繰り返し回数に個人差があることから、その出現回数を分析することによって個体を識別する方法である。本方法を用いて収集したヒト由来の培養細胞に関する調査を実施してデータを蓄積し、

“ヒト培養細胞識別データベース”を構築した。本調査研究においてヒト培養細胞には意外と多くのクロスカルチャーコンタミネーションが発生していると明らかになった。これまでJCRB細胞バンクで収集した、ヒトに由来する培養細胞数は622種であるが、そのうち33種 (約5%) にクロスカルチャーコンタミネーションが見つかったのである。この結果は詳細な実験手法を含めてJCRB細胞バンクのホームページで公開しているのでぜひ参考にしていただきたい (<http://cellbank.nibio.go.jp/> のCellIDの欄に公開している)。

3. 染色体詳細解析による細胞特性解析

JCRB細胞バンクでは、高度な染色体詳細解析技術 (mFISH法, mBand法, アレイCGH法など) を組み合わせ細胞の特性を解析している。不死化したヒト間葉系幹細胞における染色体詳細解析では、不死化のために導入した遺伝子の種類によっては、長期培養することにより非常に大きな染色体変化をもたらすことが明らかとなり、この結果は再生医療の実現を目指して様々に取り組まれている研究における基礎知見として重要であると考えられる¹⁾。また、研究に用いた染色体を詳細に解析する技術が、今後再生医療に用いられる種々の細胞の品質評価技術として発展することが期待される。

おわりに

細胞はすでに広く研究に活用される研究資源となっているが、一般の研究者は使用している細胞のマイコプラズマ汚染やクロスコンタミネーションなどの品質管理に手が回らないのが現状である。研究の再現性・信頼性向上のためにも、細胞の質に今一度注目し、細胞バンクに保存されている高品質な細胞を研究に利用されることを希望したい。

・文献

- 1) Takeuchi M, et al: *In Vitro Cell Dev Biol Anim* (2007) 43: 129-138

小原有弘 (Arihiro Kohara)

独立行政法人 医薬基盤研究所 生物資源研究部 細胞資源研究室 (JCRB細胞バンク)

E-mail: kohara@nibio.go.jp

2002年名古屋市立大学大学院薬学研究科博士課程修了、博士 (薬学)、第一化学薬品株式会社薬物動態研究所、国立医薬品食品衛生研究所変異遺伝部を経て、2005年より現所属、研究員。

水澤 博 (Hiroshi Mizusawa)

独立行政法人 医薬基盤研究所 生物資源研究部 細胞資源研究室 (JCRB細胞バンク)

E-mail: mizusawa@nibio.go.jp

わが国におけるヒト研究資源バンクの現状と今後

——JCRB (Japanese Collection of Research Bioresources) 細胞バンク (厚生労働省) から

水澤 博 (写真) 小原有弘 増井 徹

(独) 医薬基盤研究所生物資源研究部細胞資源研究室



厚生労働省研究資源バンクは、“対がん 10 年総合戦略研究”に質の高い培養細胞と遺伝子材料を提供する目的で、国立衛生試験所 (現・国立医薬品食品衛生研究所) と国立予防衛生研究所 (現・国立感染症研究所) に設置された (1985 年)。当時、癌遺伝子の発見に触発され、癌と遺伝子のかかわりに注目が集まり、一気に癌を追い詰めようという機運が高まった時期であった。

研究の推進にあたって、日本の研究体制の脆弱さがたびたび指摘されていたことから、研究材料を分譲する部門を整備して癌研究の推進が試みられたのであった。近年、研究は巨大化してスピードが求められるようになってきており、ひとりの研究者が材料の準備から実験までのすべてにかかわることは困難となり、それぞれの専門機関を育成して分業化をはかる必要があるとわが国でも考えられるようになってきたが、システムの構成力に優れるアメリカでは 1950 年代から、Coriell Institute for Medical Research (CIMR) や American Type Culture Collection (ATCC) などの細胞分譲機関を整備し、生命科学研究の推進に役立てていた。1980 年代に顕在化した経済摩擦は先進諸国に知的資産の囲い込みを促し、多くの国で研究資源バンク設置が進んだ。

わが国で研究資源バンク事業がスタートするとすぐに、培養細胞研究資源は重大な問題を抱えていることが判明した。それはマイコプラズマによる“汚染”と細胞の“誤謬”の問題であったが、研究資源バンクは単に研究材料を収集して提供するだけでなく、収集して提供するまでの間に十分な吟味を加え資源の品質を十分に見極めるところに本質的な意義があることが明らかになってきたのである。1960 年代にアメリカで顕在化したヒト培養細胞への HeLa コンタミの解決に ATCC が果たした役割からも明らかであった。著者らは日本で収集した 600 種のヒト細胞の 8% に誤謬があったことを明らかにし、日本人は器用で間違いを犯さないと信じているとしたらそれは迷信であると注意を促している。

その後、ヒトゲノムプロジェクトによりヒト遺伝子の全塩基配列が明らかにされ、細胞の品質管理法に大

きな影響を与えたが、培養細胞の誤謬を防止する目的で実施してきた遺伝子検査が細胞提供者のプライバシーを損なうかもしれないというおそれが出てきてしまったのである。現在のところ収集したヒト培養細胞は 600 種程度なので問題にはならないが、今後、生存中の方々からの試料提供を受ける必要が生じるようになると問題が顕在化すると考えられる。現在でも SNP 研究用の健常人 1,000 名分の対照実験用ゲノム DNA (PSC, JBCIC 寄託不死化血液細胞と DNA) については、そのおそれを考えて細胞の誤謬を確認するためのデータをとらないことにしている¹⁾。

さらに問題となりそうな点は、インフォームドコンセントの範囲内で利用するという考え方である。もちろん、患者さんの立場ではインフォームドコンセントで許可した以上の使い方をしてほしくないことは十分理解できるが、一方で研究というのは予想もしなかった点から新しい発見があつて、それが人類の知識を増やして疾病の治療を可能にするのである。したがって、予想外の研究に使ってはならないという規制は、研究者にとってたいへんきびしい内容で、今後議論が必要となるのではないだろうか。

現在、提供しているおもなヒト試料は論文などで公知されたものなので、心配している問題は起こらないが、今後、本特集で話題になるような細胞や移植医療に直結するようなヒト試料が多数寄託される時代がくると、こうした問題が顕在化する可能性がある。だからといって問題が指摘されるまで手をこまねいて待っているだけではわれわれに課せられた責任を果たせそうもないので、ヒト試料を扱う際に問題となりそうな倫理的課題についても研究課題と位置づけて検討を進め、ホームページ²⁾を通じて問題点を掲載し、掲示板を通じて批判的意見もいただけるようなシステムを整えている。現在、細胞バンクにヒト試料を扱うことに対する批判が直接来ているわけではないが、問題があると考えられる以上、批判をいただけるようなチャンネルを開いておくことは重要であろう。

1) 水澤 博・他：科学，71：1601-1607，2001。

2) <http://cellbank.nibio.go.jp/>

Chromosomal instability in human mesenchymal stem cells immortalized with human papilloma virus E6, E7, and hTERT genes

Masao Takeuchi · Kikuko Takeuchi · Arihiro Kohara ·
Motonobu Satoh · Setsuko Shioda · Yutaka Ozawa ·
Azusa Ohtani · Keiko Morita · Takashi Hirano ·
Masanori Terai · Akihiro Umezawa · Hiroshi Mizusawa

Received: 25 January 2007 / Accepted: 27 March 2007 / Published online: 21 May 2007 / Editor: J. Denry Sato
© The Society for In Vitro Biology 2007

Abstract Human mesenchymal stem cells (hMSCs) are expected to be an enormous potential source for future cell therapy, because of their self-renewing divisions and also because of their multiple-lineage differentiation. The finite lifespan of these cells, however, is a hurdle for clinical application. Recently, several hMSC lines have been established by immortalized human telomerase reverse transcriptase gene (hTERT) alone or with hTERT in combination with human papillomavirus type 16 E6/E7 genes (E6/E7) and human proto-oncogene, Bmi-1, but have not so much been characterized their karyotypic stability in detail during extended lifespan under in vitro conditions. In this report, the cells immortalized with the hTERT gene

alone exhibited little change in karyotype, whereas the cells immortalized with E6/E7 plus hTERT genes or Bmi-1, E6 plus hTERT genes were unstable regarding chromosome numbers, which altered markedly during prolonged culture. Interestingly, one unique chromosomal alteration was the preferential loss of chromosome 13 in three cell lines, observed by fluorescence in situ hybridization (FISH) and comparative-genomic hybridization (CGH) analysis. The four cell lines all maintained the ability to differentiate into both osteogenic and adipogenic lineages, and two cell lines underwent neuroblastic differentiation. Thus, our results were able to provide a step forward toward fulfilling the need for a sufficient number of cells for new therapeutic

M. Takeuchi (✉) · K. Takeuchi · A. Kohara · S. Shioda ·
Y. Ozawa · A. Ohtani · H. Mizusawa
Division of Bioresources,
National Institute of Biomedical Innovation,
Osaka 567-0085, Japan
e-mail: takeuchim@nibio.go.jp

K. Takeuchi
e-mail: takeuchik@nibio.go.jp

A. Kohara
e-mail: kohara@nibio.go.jp

S. Shioda
e-mail: shioda@nibio.go.jp

Y. Ozawa
e-mail: ozaway@nibio.go.jp

A. Ohtani
e-mail: ahtani@nibio.go.jp

H. Mizusawa
e-mail: mizusawa@nibio.go.jp

M. Satoh
Health Science Research Resources Bank,
Osaka 590-0535, Japan
e-mail: satoh@osa.jhsf.or.jp

K. Morita · T. Hirano · A. Umezawa
National Research Institute for Child Health and Development,
Tokyo 157-8535, Japan

K. Morita
e-mail: morita-keiko@aist.go.jp

T. Hirano
e-mail: hirano-takashi@aist.go.jp

A. Umezawa
e-mail: umezawa@1985.jukuin.keio.ac.jp

M. Terai
Department of Reproductive Biology
and Pathology and Innovative Surgery,
National Research Institute for Child Health and Development,
Tokyo 157-8535, Japan
e-mail: terai@nch.go.jp

applications, and substantiate that these cell lines are a useful model for understanding the mechanisms of chromosomal instability and differentiation of hMSCs.

Keywords Human cord blood mesenchymal stem cell · Long-term culture · Karyotype analysis · mFISH · CGH · Differentiation

Introduction

Tissue-specific stem cells in various adult tissues are known to be an important source in the regeneration of damaged tissue and maintenance of homeostasis in the tissues in which they reside. Among these stem cells, human mesenchymal stem cell (hMSC) has recently become of great interest in regenerative medicine, not only to replenish their own tissues, but also to give rise to more committed progenitor cells, which can differentiate into other tissues. MSCs in bone marrow have been shown to differentiate into several types of cell such as osteoblasts, adipocytes, chondrocytes, myocytes, and probably also neuronal cells (Okamoto et al. 2002; Takeda et al. 2004; Mori et al. 2005; Saito et al. 2005; Terai et al. 2005). Because of these properties, it is expected that hMSCs are an enormous potential source for future cell therapy. The goal of our study is to establish cell lines with long lifespan and with parental properties for clinical application. However, clinical application using these cells has been met with enormous difficulty, e.g., isolation of a cell population with specific criteria, expansion in vitro system for obtaining a sufficient number of cells without affecting their genomic characteristics and differentiation properties, and their storage in higher viability.

At present, there is a little evidence suggesting whether changes in these properties occur during expansion. Human normal MSCs have a limited capacity to replicate in the 40- to 50-population doubling level (PDL) at the most. To extend their lifespan, we have previously established human mesenchymal cell lines from human umbilical cord blood or bone marrow by immortalization with human telomerase reverse transcriptase (hTERT), human papillomavirus high-risk type 16 E6/E7 genes (HPV16E6/E7) or polycomb gene, Bmi-1 (Takeda et al. 2004; Mori et al. 2005; Terai et al. 2005).

hTERT-immortalization without affecting biological characteristics, despite extensive proliferation, has been reported in bone-marrow-derived hMSCs (Burns et al. 2005), human fibroblast (Milyavsky et al. 2003), and human keratinocyte (Harada et al. 2003), although it has been indicated that there is the possibility that prolonged culture of hTERT-immortalized fibroblasts may favor the appearance of clones carrying potentially malignant alter-

ations (Milyavsky et al. 2003). HPV16, which encodes oncogenes (E6 and E7), can also immortalize hMSCs in vitro. Both E6 and E7 proteins act through their association with tumor suppressor gene products, p53 and retinoblastoma family members (pRb), respectively. E6 accelerates the degradation of the p53 protein, which is essential for cell arrest at the checkpoint in G₁/S and at the mitotic checkpoint when tetraploidy occurs (Cross et al. 1995), as well as at the G₂ phase under damaging conditions. E7 protein binds to pRb and abrogates the repressive function of these cell cycle regulations (Zheng et al. 2001). Thus, both p53 and pRb play a multitude of important roles in cell-cycle-progression checkpoints as reported in human keratinocytes (Patel et al. 2004), and fibroblasts (Khan et al. 1998). As a consequence, the disruption of the checkpoints that govern accurate cell division leads to abnormal segregation of chromosome and genomic instability, as shown in the cells immortalized with HPV16E6/E7 genes (Duensing et al. 2002).

In this paper, we report on the chromosomal instability and the differentiation activity during prolonged culture (cell expansion) using four mesenchymal stem cell lines. These results indicate that an umbilical cord blood-derived clone immortalized with hTERT (UCBTERT-21) showed normal karyotype for a period of 1 yr, whereas three other cell lines immortalized with HPV16E6/E7 and hTERT or HPV16E6, Bmi-1 and hTERT showed chromosomal instability but maintained the ability to differentiate.

Materials and Methods

Cell culture. Human mesenchymal stem cell lines, UCB TERT-21 (JCRB1107), UCB408E6E7TERT-33 (JCRB1110), UE6E7T-3 (JCRB1136), and UBE6T-6 (JCRB1140) were obtained from the JCRB Cell Bank (Osaka, Japan). Two of them are cell lines obtained by immortalizing human umbilical cord blood mesenchymal stem cells (UCB) with hTERT alone (UCBTERT-21; Terai et al. 2005) or with HPV16E6/E7 in combination with hTERT (UCB408E6E7TERT-33; Terai et al. 2005), and the two others are human bone-marrow-derived mesenchymal stem cell lines transformed with HPV16E6/E7 and hTERT genes (UE6E7T-3; Mori et al. 2005) or with bmi-1, HPV16E6 and hTERT genes (UBE6T-6; Takeda et al. 2004; Mori et al. 2005).

The UCBTERT-21 and UCB408E6E7TERT-33 were grown in PLUSOID-M medium (Med-Shirotori Co., Tokyo, Japan) or MSCGM BulletKit (Cambrex Co., East Rutherford, NJ). UE6E7T-3 and UBE6T-6 were cultured in POWEREDBY10 medium (Med-Shirotori Co.) or MSCGM BulletKit (Cambrex Co.); 5×10^3 cells/ml of each cell line were seeded and cultured for 7–10 d. When culture